Two-fermion relativistic bound states in light-front dynamics

M. Mangin-Brinet and J. Carbonell
Institut des Sciences Nucléaires, 53, Avenida des Martyrs, 38026 Grenoble, France

V. A. Karmanov
Lebedev Physical Institute, Leninsky Prospect 53, 119991 Moscow, Russia
(Received 2 April 2003; published 24 November 2003)

In the light-front dynamics, the wave function equations and their numerical solutions, for two fermion bound systems, are presented. Analytical expressions for the ladder one-boson exchange interaction kernels corresponding to scalar, pseudoscalar, pseudovector, and vector exchanges are given. Different couplings are analyzed separately and each of them is found to exhibit special features. The results are compared with the nonrelativistic solutions.

DOI: 10.1103/PhysRevC.68.055203 PACS number(s): 11.80.Et, 11.10.St, 11.15.Tk

I. INTRODUCTION

The two-fermion system covers a huge number of applications in atomic (e^+e^-), nuclear ($NN, \bar{N}N$), and subnuclear ($q\bar{q}$) physics. The interest in using a relativistic description for such systems appeared in the early days of quantum mechanics [1,2] and has constantly been pursued since by many authors. This interest has recently found a new *élan* due to the measurements performed at Jefferson Laboratory [3–6] where simple nuclear systems have been—and are being—probed at momentum transfers much larger than their constituent masses. Consequently, this experimental activity motivated a number of works on relativistic dynamics. Extensive reviews on the past and recent deuteron results can be found in Refs. [7,8].

Most of the approaches developed for describing relativistic two-body systems are based on the Bethe-Salpeter equation [9–15] or its three-dimensional reductions of it [16–21].

An alternative approach is provided by the light-front dynamics (LFD). In its standard version, following Dirac's classification of relativistic theories [22], the state vector is defined on the $\sigma=z+t$ surface. Wave functions—defined as the Fock components of the state vector—are the formal objects of this theory and are directly comparable to their nonrelativistic counterparts. LFD has been developed and used by many authors [23–51] and represents a promising approach to nonperturbative Hamiltonian quantum field theory, especially when dealing with composite relativistic systems. The interested reader can refer to the past advances and more complete references set in the proceedings of the past conferences devoted to the subject [52,53].

The explicitly covariant version of light-front dynamics (ECLFD) was initiated by one of the present authors in a series of papers [54–56]. The state vector is there defined on a space-time hyperplane whose equation is given by $\omega\cdot x=\sigma$, where ω is a four-vector determining the orientation of the light-front plane and satisfies $\omega^2=0$. This choice is not only a mathematical *delicatesse* but a way to carry everywhere in the theory the ω dependence in an explicit way. It has several advantages, all related to the fact that ω is a four-vector with well defined transformation properties. This approach provides explicitly covariant expressions for the on shell amplitudes, a property which is often hidden in the standard formulation, recovered by fixing the value $\omega=(1,0,0,-1)$. This value is however associated to a particular reference frame and it is not valid in any other one. The formalism and some of its first applications to few-body systems have been reviewed in Ref. [57].

Approximate light-front solutions for the NN system [58,59] were found in a perturbative way over the Bonn model wave functions [60] and successfully applied to calculate the deuteron electromagnetic form factors [61] measured at Jefferson Lab. Latter applications to heavier nuclei [62,63] have shown the pertinence of this approach in describing high momentum components of the NN correlation functions.

These successes stimulated a series of works aiming at developing some formal problems of the theory and obtaining exact solutions in the ladder approximation for systems of increasing complexity. Results concerning bound states of two scalar particles can be found in Refs. [64–67].

We present in this paper the formalism and numerical solutions describing bound two-fermion systems interacting via the usual—scalar, pseudoscalar, vector, and pseudovector—one-boson exchange (OBE) kernels. Results are limited to $J=0$ and $J=1$ states. Our main interest in this work is to study the solutions of the LFD equations as they are provided by the OBE ladder sum with special interest in their stability, their comparison to the nonrelativistic limits, and the construction of nonzero angular momentum states. For this purpose, we have studied each coupling separately and the only physical system considered is positronium. The first conclusions concerning the Yukawa model have been published in Refs. [68–71] and a more detailed derivation of equations and kernels can be found in Ref. [72]. This series of works is also being extended to the two-body scattering solutions and to three-particle systems. The case of three bosons interacting via zero range forces was considered in Ref. [73]. In Refs. [74,75] the ensemble of these results is briefly reviewed.

It is worth mentioning previous works on two-fermion system using the LFD approach. In Ref. [46], the relativistic

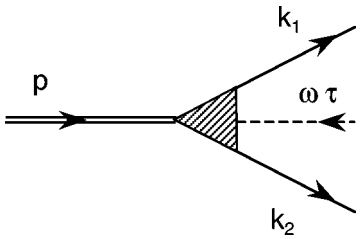

FIG. 1. Graphical representation of the light-front two-body wave function. Dashed line corresponds to the spurion (see text).

bound-state problem in the light-front Yukawa model was considered. In Refs. [37,38], positronium and heavy quarkonia calculations in discretized light cone quantization were carried out. The formalism was used in Ref. [27] to build one-boson exchange kernels and to calculate nucleon-nucleon phase shifts as well as deuteron properties. Recent application to meson spectra can be found in Refs. [40,41]. LFD was also applied in Refs. [43,45] to describe the *NN* system and nuclear matter equation of state.

The paper is organized as follows. In Sec. II we establish the structure and main properties of the explicitly covariant light-front wave functions, the two-body equation, and the OBE kernels. In Sec. III the problem of angular momentum J is discussed and states with $J=0, 1$ are constructed. In Sec. IV we derive the coupled equations for the wave function components of states with angular momentum $J=0$. The corresponding equations for $J=1$ states are derived in Sec. V. The nonrelativistic limit and perturbative calculations are discussed in Sec. VI. In Secs. VII–IX we present the results of numerical calculations. In order to disentangle their different behaviors, each coupling is separately analyzed. Section X contains a summary of the results and the concluding remarks.

II. WAVE FUNCTION, EQUATION, AND KERNELS

The wave functions we deal with are Fock components of the state vector defined on the light-front plane $\omega\cdot x=0$. For a two-fermion system—shown graphically in Fig. 1—it reads

$$\Phi_{\sigma_2\sigma_1}=\Phi_{\sigma_2\sigma_1}(k_1, k_2, p, \omega\tau), \tag{1}$$

where σ_i are the constituent angular momenta. The general form of the wave function is obtained by constructing all possible spin structures compatible with the quantum numbers of the state. The four-vector ω enters in the wave function on the same ground as the particles four-momenta, giving rise to a number of structures larger than in nonrelativistic dynamics. Each of them is mastered by a scalar function, denoted by f_i throughout the paper, which can be interpreted as a wave function component on the spin space. The number N of such independent amplitudes simply follows from the dimension of the spin matrix forming the two-fermion wave function with total momentum J, i.e., $N=\frac{1}{2}(2J+1)(2\sigma_1+1)(2\sigma_2+1)$ with a factor $\frac{1}{2}$ to take into account the parity conservation. In the case $\sigma_1=\sigma_2=\frac{1}{2}$, it gives $N=2$ amplitudes for $J=0$ states and $N=6$ for $J=1$. These wave function components will be specified in the subsequent sections.

Since the Fock-space component is, by construction, the coefficient of the state vector decomposition in the creation operators basis $a^\dagger_{\sigma_2}(\vec{k}_2)a^\dagger_{\sigma_1}(\vec{k}_1)|0\rangle$, the independent variables are the three-dimensional vectors $(\vec{k}_1, \vec{k}_2)$ and the particle energies are expressed through them. Consequently all four-momenta are on corresponding mass shells: $k_1^2=k_2^2=m^2$, $p^2=M^2$, $(\omega\tau)^2=0$ and satisfy the conservation law

$$k_1+k_2=p+\omega\tau. \tag{2}$$

This equation generalizes the $(\perp, +)$-component conservation in the standard approach; the minus components are not constrained. In the light-front coordinates with $\omega=(1, 0, 0, -1)$, the only nonzero component of ω is $\omega_-=\omega_0-\omega_z=2$. The four-vector $\omega\tau$ just incorporates the nonvanishing difference $2\tau=k_{1-}+k_{2-}-p_-$. In this sense the ECLFD wave function is off energy shell. Since the four-momentum $\omega\tau$ enters in the wave function on equal ground with the particle momenta, we associate it for convenience with a fictitious particle—called spurion—showed in Fig. 1 by a dashed line. We would like to emphasize however that the Fock-space basis does not contain, for all these, any additional and unphysical degree of freedom. By spurion, we mean only the difference—proportional to ω—between nonconserved particle four-momenta in the off-energy-shell states.

It is convenient to introduce other kinematical variables, constructed from the initial four-momenta, as follows:

$$\vec{k}=L^{-1}(\mathcal{P})\vec{k}_1=\vec{k}_1-\frac{\vec{\mathcal{P}}}{\sqrt{\mathcal{P}^2}}\left[k_{10}-\frac{\vec{k}_1\cdot\vec{\mathcal{P}}}{\sqrt{\mathcal{P}^2}+\mathcal{P}_0}\right],$$

$$\vec{n}=\frac{L^{-1}(\mathcal{P})\vec{\omega}}{|L^{-1}(\mathcal{P})\vec{\omega}|}, \tag{3}$$

where $\mathcal{P}=p+\omega\tau$ and $L^{-1}(\mathcal{P})$ results from the Lorentz boost into the reference system where $\vec{\mathcal{P}}=0$. In these variables wave function (1) is represented as

$$\Phi_{\sigma_2\sigma_1}=\Phi_{\sigma_2\sigma_1}(\vec{k}, \vec{n}). \tag{4}$$

Under rotations and Lorentz transformations of four-momenta $k_1, k_2, p, \omega\tau$, variables $(\vec{k}, \vec{n})$ are only rotated, so the three-dimensional parametrization (4) is also explicitly covariant. In practice, instead of the formal transformations (3), it is enough to consider the wave function and the equation in the center-of-mass (c.m.) system where $\vec{\mathcal{P}}=\vec{k}_1+\vec{k}_2=0$ and set $\vec{k}_1=\vec{k}$, $\vec{k}_2=-\vec{k}$, $\vec{\omega}=\vec{n}|\vec{\omega}|$. Because of covariance, the result is the same as after transformation (3). Since $\vec{\omega}$ determines only the orientation of the light-front plane, the modulus $|\vec{\omega}|$ disappears from the wave functions and amplitudes. Note that in the c.m. system, the momentum $\vec{p}$ is not zero: $\vec{p}=-\vec{\omega}\tau$.

The light-front graph technique is a covariant generalization of the old fashioned perturbation theory. The latter was developed by Kadyshevsky [77] and adapted to the explicitly covariant version in Refs. [54,57].

The equation for the wave function is shown graphically in Fig. 2. It is the projection on the two-body sector of the general mass equation $P^2\phi=M^2\phi$. Its analytical form is ob-

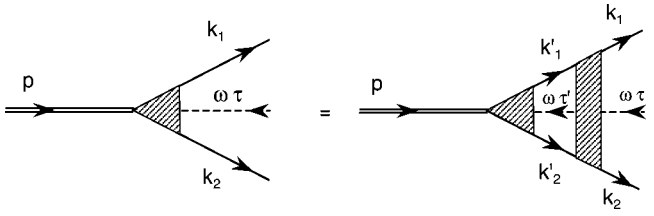

FIG. 2. Equation for the two-body wave function.

tained by applying the rules of the graph techniques to the diagrams in Fig. 2. In variables (3) this equation reads

$$[4(k^2+m^2)-M^2]\Phi_{\sigma_2\sigma_1}(\vec{k},\vec{n}) = -\frac{m^2}{2\pi^3}\int \sum_{\sigma_1'\sigma_2'} K^{\sigma_2'\sigma_1'}_{\sigma_2\sigma_1}(\vec{k},\vec{k}',\vec{n},M^2)\Phi_{\sigma_2'\sigma_1'}(\vec{k}',\vec{n})\frac{d^3k'}{\varepsilon_{k'}}, \tag{5}$$

where $K^{\sigma_2'\sigma_1'}_{\sigma_2\sigma_1}(\vec{k},\vec{k}',\vec{n},M^2)$ is the interaction kernel. We detail in what follows the LFD one-boson exchange kernels corresponding to the interaction Lagrangians.

(i) Scalar (S):

$$\mathcal{L}^{int} = g_s\bar{\psi}\psi\phi^{(s)}. \tag{6}$$

(ii) Pseudoscalar (PS):

$$\mathcal{L}^{int} = ig_{ps}\bar{\psi}\gamma_5\psi\phi^{(ps)}. \tag{7}$$

(iii) Pseudovector (PV):

$$\mathcal{L}^{int} = -\frac{f_{pv}}{2m}\bar{\psi}\gamma^\mu\gamma_5\psi\partial_\mu\phi^{(ps)}. \tag{8}$$

(iv) Vector (V):

$$\mathcal{L}^{int} = \bar{\psi}\left[g_v\gamma^\mu\phi^{(v)}_\mu + \frac{f_t}{4m}\sigma^{\mu\nu}(\partial_\mu\phi^{(v)}_\nu - \partial_\nu\phi^{(v)}_\mu)\right]\psi. \tag{9}$$

with

$$\sigma^{\alpha'\alpha} = \frac{i}{2}(\gamma^{\alpha'}\gamma^\alpha - \gamma^\alpha\gamma^{\alpha'}).$$

The LFD ladder kernels have two contributions corresponding to the two time-ordered diagrams (in the light-front time) shown in Fig. 3. For S, PS, and PV couplings they have the structure

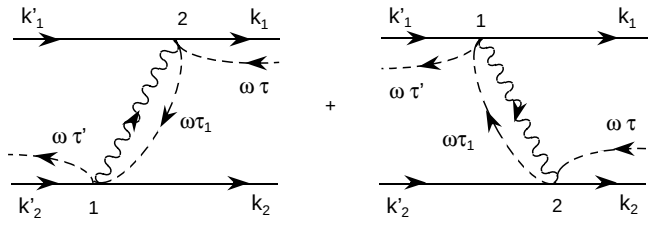

FIG. 3. One-boson exchange kernel.

$$K^{\sigma_2'\sigma_1'}_{\sigma_2\sigma_1}(k_1,k_2,\omega\tau;k_1',k_2',\omega\tau') = -\frac{1}{4m^2}[\bar{u}^{\sigma_2}(k_2)O_2u^{\sigma_2'}(k_2')] \times[\bar{u}^{\sigma_1}(k_1)O_1u^{\sigma_1'}(k_1')] \times\left\{\frac{\theta(\omega\cdot(k_1'-k_1))}{\mu^2-(k_1'-k_1)^2+2\tau'\omega\cdot(k_1'-k_1)} + \frac{\theta(\omega\cdot(k_1-k_1'))}{\mu^2-(k_1-k_1')^2+2\tau\omega\cdot(k_1-k_1')}\right\}. \tag{10}$$

For scalar exchange

$$O_1 = O_2 = g_s,$$

for pseudoscalar

$$O_1 = O_2 = i\gamma_5 g_{ps},$$

and for pseudovector

$$O_1 = \begin{cases}\left(1-\dfrac{\hat{\omega}\tau}{2m}\right)i\gamma_5 f_{pv} \text{ if } \omega\cdot(k_1-k_1')>0\\ \left(1+\dfrac{\hat{\omega}\tau'}{2m}\right)i\gamma_5 f_{pv} \text{ if } \omega\cdot(k_1-k_1')<0,\end{cases}$$

$$O_2 = \begin{cases}\left(1+\dfrac{\hat{\omega}\tau'}{2m}\right)i\gamma_5 f_{pv} \text{ if } \omega\cdot(k_1-k_1')>0\\ \left(1-\dfrac{\hat{\omega}\tau}{2m}\right)i\gamma_5 f_{pv} \text{ if } \omega\cdot(k_1-k_1')<0,\end{cases}$$

with

$$\tau = \frac{4\varepsilon_k^2-M^2}{2\omega\cdot p}, \quad \tau' = \frac{4\varepsilon_{k'}^2-M^2}{2\omega\cdot p}.$$

For values $\tau,\tau'\neq 0$ the kernels are off-energy shell. In this case the pseudoscalar and pseudovector kernels differ from each other but coincide on energy shell ($\tau=\tau'=0$).

We use the notation $\hat{\omega}=\omega_\mu\gamma^\mu$. Writing the propagators in the c.m. variables, Eq. (10) gets the simpler form

$$K^{\sigma_2'\sigma_1'}_{\sigma_2\sigma_1} = -\frac{1}{4m^2}\frac{1}{Q^2+\mu^2}[\bar{u}_{\sigma_2}(k_2)O_2u_{\sigma_2'}(k_2')][\bar{u}_{\sigma_1}(k_1)O_1u_{\sigma_1'}(k_1')], \tag{11}$$

with

$$Q^2 = (\vec{k}-\vec{k}')^2 - (\vec{k}\cdot\vec{n})(\vec{k}'\cdot\vec{n})\frac{(\varepsilon_k-\varepsilon_{k'})^2}{\varepsilon_k\varepsilon_{k'}} + \left(\varepsilon_k^2+\varepsilon_{k'}^2-\frac{1}{2}M^2\right) \times \left|\frac{\vec{k}\cdot\vec{n}}{\varepsilon_k}-\frac{\vec{k}'\cdot\vec{n}}{\varepsilon_{k'}}\right|. \tag{12}$$

The kernel for the vector coupling is given by a contraction of terms similar to Eq. (11) with the tensor structures $L_{\alpha\beta}$. It reads

$$K^{\sigma_2'\sigma_1'}_{\sigma_2\sigma_1} = -\frac{1}{4m^2}\frac{1}{\mu^2+Q^2}L_{\alpha\beta}[\bar{u}(k_1)O_1^\alpha u(k_1')][\bar{u}(k_2)O_2^\beta u(k_2')], \tag{13}$$

with

$$L_{\alpha\beta} = \begin{cases} -g_{\alpha\beta}+\dfrac{1}{\mu^2}(k_1-k_1'-\omega\tau)_\alpha(k_2'-k_2-\omega\tau')_\beta \text{ if } \omega\cdot(k_1-k_1')>0 \\ -g_{\alpha\beta}+\dfrac{1}{\mu^2}(k_1'-k_1-\omega\tau')_\alpha(k_2-k_2'-\omega\tau)_\beta \text{ if } \omega\cdot(k_1-k_1')<0 \end{cases} \tag{14}$$

and vertex operators

$$O_1^\alpha = \begin{cases} g_v\gamma^\alpha+\dfrac{f_t}{2m}\sigma^{\alpha'\alpha}(-i)(k_1-k_1'-\omega\tau)_{\alpha'} \text{ if } \omega\cdot(k_1-k_1')>0 \\ g_v\gamma^\alpha+\dfrac{f_t}{2m}\sigma^{\alpha'\alpha}(i)(k_1'-k_1-\omega\tau')_{\alpha'} \text{ if } \omega\cdot(k_1-k_1')<0, \end{cases} \tag{15}$$

$$O_2^\beta = \begin{cases} g_v\gamma^\beta+\dfrac{f_t}{2m}\sigma^{\beta'\beta}(i)(k_2'-k_2-\omega\tau')_{\beta'} \text{ if } \omega\cdot(k_1-k_1')>0 \\ g_v\gamma^\beta+\dfrac{f_t}{2m}\sigma^{\beta'\beta}(-i)(k_2-k_2'-\omega\tau)_{\beta'} \text{ if } \omega\cdot(k_1-k_1')<0. \end{cases} \tag{16}$$

Hereafter we will not take into account the tensor coupling, that is, we put $f_t=0$ and $O_1^\alpha=O_2^\alpha=g_v\gamma^\alpha$. In this case, vector kernel (13) simplifies into

$$K^{\sigma_2'\sigma_1'}_{\sigma_2\sigma_1} = \frac{g_v^2}{4m^2}\frac{1}{\mu^2+Q^2}\left\{[\bar{u}(k_1)\gamma^\alpha u(k_1')][\bar{u}(k_2)\gamma_\alpha u(k_2')] - \frac{\tau\tau'}{\mu^2}[\bar{u}(k_1)\hat{\omega}u(k_1')][\bar{u}(k_2)\hat{\omega}u(k_2')]\right\}. \tag{17}$$

In the $\mu=0$ case, e.g., one-photon or one-gluon exchange kernels, the $L_{\alpha\beta}$ expressions depend on the gauge. Using the Feynman gauge, one has $L_{\alpha\beta}=-g_{\alpha\beta}$, i.e., the μ-dependent terms in Eq. (14) and (17) are simply dropped out.

It will often be necessary to regularize the LFD kernels by means of vertex form factors. Unless the contrary is explicitly mentioned, we will take the form used in the Bonn model [60], i.e.,

$$F(Q^2) = \left(\frac{\Lambda^2-\mu^2}{\Lambda^2+Q^2}\right)^n, \tag{18}$$

where Λ and n are parameters whose values depend on the coupling. Form factors appear in the kernels multiplying each of the vertex operators O_i. In the nonrelativistic limit, $Q^2\approx(\vec{k}-\vec{k}')^2$ and F is local in configuration space. This locality is however broken from the very beginning in LFD due to the $\vec{n}$-dependent terms on Q^2.

III. ANGULAR MOMENTUM

In LFD the construction of states with definite angular momentum is a delicate problem. Working in the explicitly covariant version, we have developed a method to overcome this difficulty. It will be explained in this section. In contrast to the equal-time approach, the LFD generators $J_{\rho\gamma}=J^0_{\rho\gamma}+J^{int}_{\rho\gamma}$ of four-dimensional rotations are not kinematical, but contain interaction in $J^{int}_{\rho\gamma}$. The interaction also enters in the angular momentum operator, i.e., the Pauli-Lubansky vector

$$S_\mu = \tfrac{1}{2}\varepsilon_{\mu\nu\rho\gamma}P^\nu J^{\rho\gamma}. \tag{19}$$

Just as the action of the Hamiltonian on the Schrödinger wave function is expressed through the time derivative

$$H^{int}\phi = i\partial_t\phi,$$

the action of $J^{int}_{\rho\gamma}$ on the LFD state vector is expressed through derivatives with respect to the four-vector ω [78]:

$$J^{int}_{\mu\nu}\ \phi(\omega) = L_{\mu\nu}(\omega)\phi(\omega), \tag{20}$$

where

$$L_{\mu\nu}(\omega) = i\left(\omega_\mu \frac{\partial}{\partial\,\omega^\nu} - \omega_\nu \frac{\partial}{\partial\,\omega^\mu}\right). \tag{21}$$

Equation (20) is called *angular condition* and can also be written in the form

$$S_\mu\ \phi(\omega) = W_\mu\ \phi(\omega) \tag{22}$$

with

$$W_\mu = \tfrac{1}{2}\epsilon_{\mu\nu\rho\gamma}P^\nu M^{\rho\gamma} \tag{23}$$

and

$$M_{\mu\nu} = J^0_{\mu\nu} + L_{\mu\nu}(\omega).$$

W_μ is a kinematical Pauli-Lubansky vector. As long as the angular condition is satisfied, the dynamical Pauli-Lubansky vector S_μ can be replaced by the kinematical one W_μ. The great benefit of doing so is that the problem of constructing angular momentum states with operator (23) becomes purely kinematical. In practice, one rather prefers to start constructing states with definite angular momentum using W_μ, and then take into account the restriction imposed by the angular condition (20).

It is worth noting that without this condition there is an ambiguity in defining the state vector with given angular momentum. This can be seen by introducing the operator

$$\hat{A}^2 = \left(\frac{W\cdot\omega}{P\cdot\omega}\right)^2. \tag{24}$$

It commutes with P_μ and W_μ and—taking A^2 instead of A—with the parity operator. The state vector is then characterized not only by its mass M^2, momentum p, angular momentum J—defined by means of Eq. (23)—and parity π but also by a, the square root of the A^2 eigenvalue,

$$\hat{A}^2\phi^{(a)} = a^2\phi^{(a)}. \tag{25}$$

For a total angular momentum J there are $J+1$ eigenstates $\phi^{(a)}$. In principle one could imagine any of these eigenstates to be an acceptable solution. It turns out however that, except for $J=0$, none of these eigenstates can satisfy the angular condition (22). Indeed if $\phi(\omega)$ is an eigenstate of A^2, the right hand side of Eq. (22)—$W_\mu\phi(\omega)$—is still an eigenstate of A^2 whereas this is not possible on its left hand side—$S_\mu\phi(\omega)$—due to the nonzero commutator $[S_\mu, A^2]\neq 0$. What is then the state vector?

A solution of the angular condition— the only remaining equation to be fulfilled—is therefore provided by a linear combination of different eigenstates $\phi^{(a)}$:

$$\phi = \sum_{a=0}^{J} c_a\ \phi^{(a)}. \tag{26}$$

The coefficients c_a can in principle be determined by inserting Eq. (26) into Eqs. (20) and (22).

We would like to emphasize this result, which is, to our opinion, an important issue of light-front dynamics. It tells us that the state vector is necessarily a superposition of different A^2 eigenstates. This conclusion does not depend on the approximation resulting from any eventual Fock-space truncation.

In an exact solution of the problem, i.e., with the generators satisfying the Poincaré algebra, the eigenstates $\phi^{(a)}$ are degenerate in mass and superposition (26) is furthermore a solution of the mass equation (5). Indeed, as already noticed, $S_\mu\phi^{(a)}$ is not an eigenstate of A^2 but a superposition of different A^2 eigenstates. On the other hand, the commutation relation $[S_\mu, P_\nu]=0$ implies $S_\mu\phi^{(a)}$ to have the same mass as $\phi^{(a)}$. This is possible only if the masses of different states $\phi^{(a)}$ are equal.

Due to the Fock-space truncation, or some other kind of approximation, the Poincaré algebra is violated. The eigenstates $\phi^{(a)}$ are no longer degenerate and solution (26), built with eigenstates of different mass, cannot satisfy Eq. (5). However, while this equation is an approximate one, form (26) for the state vector remains valid. Each term in Eq. (31) is an exact solution of the truncated mass equation (5) with eigenvalue M_a^2. Their superposition does not satisfy any mass equation but has the proper form of the nontruncated Hamiltonian problem. The corresponding mass squared—at the same level of approximation—is given by

$$M^2 = \sum_{a=0}^{J} c_a^2 M_a^2. \tag{27}$$

The ensemble (ϕ, M) obtained in this way constitutes the solution of the problem compatible with the degree of approximation considered.

This formalism is translated to $J=1$ states in the two-body sector as follows. The interaction kernel $K(\vec{k}', \vec{k}, \vec{n}, M)$ depends on scalar products of vectors $\vec{k}', \vec{k}, \vec{n}$ and also on scalar products with Pauli matrices $\vec{k}\cdot\vec{\sigma}, \vec{k}'\cdot\vec{\sigma}, \vec{n}\cdot\vec{\sigma}$. Therefore the total angular momentum operator constructed as

$$\vec{J} = -i[\vec{k}\times\partial_{\vec{k}}] - i[\vec{n}\times\partial_{\vec{n}}] + \vec{s}_1 + \vec{s}_2 \tag{28}$$

commutes with the kernel ($\vec{s}_{1,2}$ are the fermion spin operators). In the c.m. system this operator is proportional to the kinematical Pauli-Lubansky vector $\vec{W}$ given in Eq. (23). The solutions of Eq. (5) correspond to definite J and J_z eigenvalues of the operators $\vec{J}^2, J_z$.

Since A^2 is applied to states with definite p, it has the form

$$A^2 = (\vec{n}\cdot\vec{J})^2. \tag{29}$$

A^2 commutes with the kernel K since $\vec{J}$ commutes with K and $\vec{n}$ is a parameter. It commutes also with $\vec{J}$ since A is a scalar. Thus, as in the case of a full state vector (25), the truncated solutions in the two-body sector are also labeled by a:

$$A^2\vec{\psi}^{(a)}(\vec{k},\vec{n}) = a^2\vec{\psi}^{(a)}(\vec{k},\vec{n}), \tag{30}$$

and the two-body wave function is a superposition of A^2 eigenstates $\vec{\psi}^{(a)}$ with different a values:

$$\vec{\psi}(\vec{k},\vec{n}) = c_0\vec{\psi}^{(0)}(\vec{k},\vec{n}) + c_1\vec{\psi}^{(1)}(\vec{k},\vec{n}). \tag{31}$$

The mass equations determining the eigenstates $\vec{\psi}^{(a)}$ with different a are decoupled; in particular, the $J=0$ state is determined by one single equation. We would like to comment here that the decoupling into subsystems takes place in any formulation of LFD, both in the explicitly covariant and in the standard one. However, in the latter approach it looks as a *matter of art*, whereas in ECLFD this splitting has transparent reasons. For example, in Ref. [46] the four-equation system for the wave function components with angular momentum projection $m=0$ was split, by a proper transformation, into two subsystems with two equations each. In ECLFD this corresponds to the $a=0$ eigenstate of $J=0$ and $J=1$ states, each of them having two components.

Because of the truncation of the Fock space, the states $\vec{\psi}^{(a)}$ are not degenerate. Their splitting was effectively calculated in the case of scalar particles in Refs. [44,65,66] for $J=1,2$ as a function of the coupling constant. It has been shown in Ref. [44] that this splitting indeed decreased when the interaction kernel incorporates a larger number of particles in the intermediate states. However, the number of states taken into account in any practical calculation will be always very limited. The splitting, though decreased, will remain, especially for strongly bound systems such as $q\bar{q}$ mesons. The problem of determining the state vector at a given level of approximation is thus not solved by this way. These are some of the reasons why, as explained before, our approach to dealing with this problem follows a different philosophy. Despite the nondegeneracy of $\vec{\psi}^{(a)}$, we search the physical two-body wave function in form (31), the same as for the full state vector (26). The corresponding mass squared is given by

$$M^2 = c_0^2M_0^2 + c_1^2M_1^2, \tag{32}$$

where M_a^2 is the mass associated with $\vec{\psi}^{(a)}$. The M^2 value thus obtained is always between M_0^2 and M_1^2, where the exact solution would be.

To determine in practice coefficients c_a, we use a method proposed in Refs. [65,66,72], without explicitly solving Eq. (20). It is based on the fact that, when the momentum $k \to 0$, the interaction part in Eq. (20) is irrelevant and the angular condition reads simply $L_{\mu\nu}\phi=0$. Thus, in this limit, $\vec{\psi}$ does not depend on the light-front direction $\vec{n}$ anymore. Such a requirement unambiguously determines the coefficients of the superposition. The method was applied to a model with scalar particles [66] and found to give very accurate results. The procedure will be detailed in Sec. V and illustrated by numerical calculations in Sec. VII.

IV. $J=0$ STATES

The $J=0^+$ two-fermion wave function can be written in the form [59,57]

$$\Phi_{\sigma_2\sigma_1}(k_1,k_2,p,\omega\tau) = \sqrt{m}\bar{u}_{\sigma_2}(k_2)\phi U_c\bar{u}_{\sigma_1}(k_1), \tag{33}$$

where

$$u_\sigma(k) = \sqrt{\varepsilon_k+m}\begin{pmatrix} 1 \\ \dfrac{\vec{\sigma}\cdot\vec{k}}{(\varepsilon_k+m)} \end{pmatrix} w_\sigma \tag{34}$$

is the Dirac spinor normalized to $\bar{u}_\sigma u_{\sigma'} = 2m\delta_{\sigma\sigma'}$, w_σ the Pauli spinor normalized to $w_\sigma^\dagger w_{\sigma'} = \delta_{\sigma\sigma'}$, and $\varepsilon_k = \sqrt{\vec{k}^{\,2}+m^2}$. $U_c = \gamma^2\gamma^0$ is the charge conjugation matrix. In its turn, ϕ is written as a superposition of two independent spin structures S_i,

$$S_1 = \frac{1}{2\sqrt{2}\varepsilon_k}\gamma_5, \tag{35}$$

$$S_2 = \frac{\varepsilon_k}{2\sqrt{2}mk\sin\theta}\left(\frac{2m}{\omega\cdot p}\hat{\omega} - \frac{m^2}{\varepsilon_k^2}\right)\gamma_5,$$

whose coefficients f_i, scalar functions depending on variables $(k, \cos\theta = \vec{n}\cdot\vec{k}/k)$, are the wave function components in the spin-space:

$$\phi = f_1S_1 + f_2S_2. \tag{36}$$

The existence of one additional component with respect to the nonrelativistic theory is due to the $\hat{\omega}=\omega_\mu\gamma^\mu$ term. The number of independent amplitudes determining the wave function is however the same, whatever be the LFD version used. We have shown in a preceding work [68] that the $J^\pi = 0^+$ state we are considering is strictly equivalent in the standard approach to the $(1+,2-)$ one [46], which is described also by two components Φ^{1+}, Φ^{2-}.

In the reference system where $\vec{k}_1+\vec{k}_2=0$ wave function (33) takes the form

$$\Phi_{\sigma_2\sigma_1} = \sqrt{m}w_{\sigma_2}^\dagger\psi(\vec{k},\vec{n})w_{\sigma_1}^\dagger, \tag{37}$$

with

$$\psi(\vec{k},\vec{n}) = \frac{1}{\sqrt{2}}\left(f_1 + \frac{i\vec{\sigma}\cdot[\vec{k}\times\vec{n}]}{k\sin\theta}f_2\right)\sigma_y. \tag{38}$$

The definition of the components themselves is to some extent arbitrary, as are the choices of structures (35). Our choice (35) is justified by the clear separation of $\vec{n}$-independent and -dependent terms it induces in wave function (38).

The normalization condition reads

$$\begin{aligned}
&\frac{1}{(2\pi)^3}\sum_{\sigma_2\sigma_1}\int|\Phi_{\sigma_2\sigma_1}|^2\frac{d^3k}{\varepsilon_k} \\
&= \frac{m}{(2\pi)^3}\int \mathrm{Tr}\{\bar{\phi}(\hat{k}_2+m)\phi(\hat{k}_1-m)\}\frac{d^3k}{\varepsilon_k} \\
&= \frac{m}{(2\pi)^3}\int \mathrm{Tr}\{\psi^\dagger(\vec{k},\vec{n})\psi(\vec{k},\vec{n})\}\frac{d^3k}{\varepsilon_k} \\
&= \frac{m}{(2\pi)^3}\int (f_1^2+f_2^2)\frac{d^3k}{\varepsilon_k} = 1,
\end{aligned} \tag{39}$$

where we denote $\overline{\phi}=\gamma_0\phi^\dagger\gamma_0$. The spin structures S_i introduced in Eq. (35) are orthonormalized relative to the trace

$$\mathrm{Tr}\{\overline{S}_i(\hat{k}_2+m)S_j(\hat{k}_1-m)\}=\delta_{ij}, \tag{40}$$

where $\overline{S}_i=\gamma_0 S_i^\dagger\gamma_0$, that is

$$\overline{S}_1=-\frac{1}{2\sqrt{2}\varepsilon_k}\gamma_5,$$

$$\overline{S}_2=-\frac{\varepsilon_k}{2\sqrt{2}mk\,\sin\theta}\gamma_5\left(\frac{2m\hat{\omega}}{\omega\cdot p}-\frac{m^2}{\varepsilon_k^2}\right). \tag{41}$$

Substituting in Eq. (5) wave function (33), multiplying it on the left by $u(k_2)$, on the right by $u(k_1)$, and using relation $\Sigma_\sigma u^\sigma(k)\overline{u}^\sigma(k)=\hat{k}+m$, we find

$$\begin{aligned}&[4(\vec{k}^2+m^2)-M^2](\hat{k}_2+m)\phi(\hat{k}_1-m)\\&\quad=-\frac{m^2}{2\pi^3}\int\frac{1}{4m^2(Q^2+\mu^2)}(\hat{k}_2+m)O_2(\hat{k}_2'+m)\phi'\\&\qquad\times(\hat{k}_1'-m)\widetilde{O}_1(\hat{k}_1-m)\frac{d^3k'}{\varepsilon_{k'}},\end{aligned} \tag{42}$$

with $\widetilde{O}=U_cO^tU_c$. Replacing ϕ here by its decomposition (36), multiplying Eq. (42) by $\overline{S}_i$, and using the orthogonality relations (40), we end up with a two-dimensional integral equation system for components f_i:

$$\begin{aligned}&[4(k^2+m^2)-M^2]f_i(k,\theta)\\&\quad=-\frac{m^2}{2\pi^3}\sum_{j=1,2}\int K_{ij}(k,\theta;k',\theta')f_j(k',\theta')\frac{d^3k'}{\varepsilon_{k'}}.\end{aligned} \tag{43}$$

Its solution will directly provide the mass of the $J^\pi=0^+$ state.

Kernels K_{ij} appearing in Eq. (43) result from integrating kernels κ_{ij} over the azimuthal angle φ:

$$K_{ij}=\frac{1}{m^2\varepsilon_k\varepsilon_{k'}}\int_0^{2\pi}\frac{\kappa_{ij}}{Q^2+\mu^2}\quad\frac{d\varphi'}{2\pi}, \tag{44}$$

with Q^2 defined in Eq. (12). For S, PS, and PV couplings $\widetilde{O}_1=U_cO_1^tU_c=O_1$ and κ_{ij} are given by

$$\kappa_{ij}=\tfrac{1}{4}\varepsilon_k\varepsilon_k'\mathrm{Tr}[\overline{S}_i(\hat{k}_2+m)O_2(\hat{k}_2'+m)S'_j(\hat{k}_1'-m)O_1(\hat{k}_1-m)]. \tag{45}$$

We denote by S_j' the quantities (35) as a function of primed arguments. For vector exchange

$$\begin{aligned}\kappa_{ij}=&-\tfrac{1}{4}\varepsilon_k\varepsilon_k'L_{\alpha\beta}\mathrm{Tr}[\overline{S}_i(\hat{k}_2+m)O_2^\alpha(\hat{k}_2'+m)S'_j(\hat{k}_1'-m)O_1^\beta\\&\times(\hat{k}_1-m)].\end{aligned} \tag{46}$$

Tensor $L_{\alpha\beta}$ is defined in Eq. (14) and we have taken into account that for V coupling $\widetilde{O}_1=U_cO_1^tU_c=-O_1$. The analytic expressions of κ_{ij} for S, PS, PV, and V exchanges are given in Appendix A.

One would remark that we have kept, for convenience, a three-dimensional volume element in Eq. (43) despite the fact that kernels K_{ij} as well as amplitudes f_j are independent of variable φ'.

V. $J=1$ STATES

In a similar way as in Eq. (33), the $J=1^+$ two-fermion wave function can be written in the form [56,58]

$$\Phi^\lambda_{\sigma_2\sigma_1}(k_1,k_2,p,\omega\tau)=\sqrt{m}e_\mu(p,\lambda)\overline{u}^{\sigma_2}(k_2)\phi^\mu U_c\overline{u}^{\sigma_1}(k_1), \tag{47}$$

where $e_\mu(p,\lambda)$ is the polarization vector. ϕ^μ develops over the six spin structures

$$\begin{aligned}&S_{1\mu}=\frac{(k_1-k_2)^\mu}{2m^2},\quad S_{2\mu}=\frac{1}{m}\gamma^\mu,\\&S_{3\mu}=\frac{\omega^\mu}{\omega\,.\,p},\quad S_{4\mu}=\frac{(k_1-k_2)^\mu\hat{\omega}}{2m\omega\cdot p},\\&S_{5\mu}=-\frac{i}{m^2\omega\cdot p}\gamma_5\epsilon^{\mu\nu\rho\gamma}k_{1\nu}k_{2\rho}\omega_\gamma,\quad S_{6\mu}=\frac{m\omega^\mu\hat{\omega}}{(\omega\cdot p)^2},\end{aligned} \tag{48}$$

with components φ_i, invariant functions depending on the same scalar variables as for $J=0$,

$$\phi^\mu=\varphi_1S_{1\mu}+\varphi_2S_{2\mu}+\varphi_3S_{3\mu}+\varphi_4S_{4\mu}+\varphi_5S_{5\mu}+\varphi_6S_{6\mu}. \tag{49}$$

In the reference system $\vec{k}_1+\vec{k}_2=0$ this wave function takes the form

$$\vec{\Psi}_{\sigma_2\sigma_1}(\vec{k},\vec{n})=\sqrt{m}w^\dagger_{\sigma_2}\vec{\psi}(\vec{k},\vec{n})\sigma_yw^\dagger_{\sigma_1}, \tag{50}$$

with

$$\begin{aligned}\vec{\psi}(\vec{k},\vec{n})=&f_1\frac{1}{\sqrt{2}}\vec{\sigma}+f_2\frac{1}{2}\left(\frac{3\vec{k}(\vec{k}\cdot\vec{\sigma})}{\vec{k}^2}-\vec{\sigma}\right)+f_3\frac{1}{2}[3\vec{n}(\vec{n}\cdot\vec{\sigma})-\vec{\sigma}]\\&+f_4\frac{1}{2k}[3\vec{k}(\vec{n}\cdot\vec{\sigma})+3\vec{n}(\vec{k}\cdot\vec{\sigma})-2(\vec{k}\cdot\vec{n})\vec{\sigma}]\\&+f_5\sqrt{\frac{3}{2}}\frac{i}{k}[\vec{k}\times\vec{n}]+f_6\frac{\sqrt{3}}{2k}[\vec{n}(\vec{k}\cdot\vec{\sigma})-\vec{k}(\vec{n}\cdot\vec{\sigma})].\end{aligned} \tag{51}$$

Contrary to the $J=0$ case, components f_i appearing in Eq. (51) are not the same as φ_i from Eq. (49). Their relation is given in Appendix B. Components $f_{3,4,5,6}$, driving $\vec{n}$-dependent spin structures, are of relativistic origin and are absent in a nonrelativistic approach.

As explained in Sec. III, the system of equations determining the six components f_i is split into two subsystems, corresponding to the eigenvalues $a=0,1$ of $\hat{A}^2$ (29). As for the $J=0$ wave function, the $J=1, a=0$ eigenstate is determined by two components whereas the remaining four correspond to $J=1, a=1$. We would like to note that the total

number of components as well as the dimension of decoupled subsystems (2+4) coincide with what is found in the standard approach [46].

The components determining the eigenstates $\vec{\psi}^{(a)}$ of A^2 will be denoted by $g^{(a=0)}_{i=1,2}$ and $g^{(a=1)}_{i=1,2,3,4}$. They are indeed different from f_i appearing in wave function (51) though g's fully determine f's by linear combinations. In view of constructing superposition (31) it is convenient to represent the eigenfunctions $\vec{\psi}^{(a)}$ in the form of Eq. (51). Only some of the six $f^{(a)}_i$ involved components will be independent— two for the $a=0$ state and four for $a=1$—but this way will facilitate further analysis.

In the following two sections we will explicitly construct the eigenfunctions $\vec{\psi}^{(a)}$ of the kinematical operator A^2, obtain the corresponding mass equation (5) in terms of $g^{(a)}_i$, and relate them with components $f^{(a)}_i$ defined in Eq. (51).

A. $a=0$

One can check from Eq. (30) that $\vec{\psi}^{(0)}$ is parallel to $\vec{n}$, i.e., it satisfies $\vec{\psi}^{(0)}=\vec{n}(\vec{n}\cdot\vec{\psi}^{(0)})$, and has the following general decomposition:

$$\vec{\psi}^{(0)}(\vec{k},\vec{n})=\sqrt{\frac{3}{2}}\left\{g^{(0)}_1\frac{\vec{\sigma}\cdot\vec{k}}{k}+g^{(0)}_2\frac{\vec{\sigma}\cdot(\vec{k}\cos\theta-k\vec{n})}{k\sin\theta}\right\}\vec{n}. \tag{52}$$

It can be written in form (51) by defining the $f^{(0)}_i$ components

$$f^{(0)}_1=\frac{1}{\sqrt{3}}\cos\theta g^{(0)}_1-\frac{1}{\sqrt{3}}\sin\theta g^{(0)}_2,$$

$$f^{(0)}_2=0,$$

$$f^{(0)}_3=-\frac{\sqrt{2}}{\sqrt{3}\sin\theta}g^{(0)}_2,$$

$$f^{(0)}_4=\frac{1}{\sqrt{6}}g^{(0)}_1+\frac{1}{\sqrt{6}}\cot\theta g^{(0)}_2,$$

$$f^{(0)}_5=0,$$

$$f^{(0)}_6=\frac{1}{\sqrt{2}}g^{(0)}_1+\frac{1}{\sqrt{2}}\cot\theta g^{(0)}_2, \tag{53}$$

that is, four nonzero components, with only two of them being independent. It can also be represented in a four-dimensional form similar to Eq. (49),

$$\phi^{(0)}_\mu=f^{(0)}_1S^{(0)}_{1\mu}+f^{(0)}_2S^{(0)}_{2\mu} \tag{54}$$

by introducing the spin structures $S^{(0)}_{i\mu}$,

$$S^{(0)}_{1\mu}=\frac{\sqrt{3}M}{2\sqrt{2}k}S_{3\mu}, \tag{55}$$

$$S^{(0)}_{2\mu}=\frac{\sqrt{3}M}{m\sqrt{2}\sin\theta}\left(\frac{m^2\cos\theta}{2\varepsilon_k k}S_{3\mu}+S_{6\mu}\right), \tag{56}$$

with $S_{i\mu}$ defined in Eq. (48).

The normalization condition is

$$\begin{aligned}\frac{1}{3(2\pi)^3}\sum_{\lambda\sigma_2\sigma_1}\int|\Phi^{\lambda}_{\sigma_2\sigma_1}|^2\frac{d^3k}{\varepsilon_k}&=\frac{m}{(2\pi)^3}\int\Pi^{\mu\nu}\mathrm{Tr}\{\phi^{(0)}_\mu(\hat{k}_2+m)\phi^{(0)}_\nu(\hat{k}_1-m)\}\frac{d^3k}{\varepsilon_k}\\&=\frac{m}{3(2\pi)^3}\int\mathrm{Tr}\{\vec{\psi}^{(0)\dagger}(\vec{k},\vec{n})\vec{\psi}^{(0)}(\vec{k},\vec{n})\}\frac{d^3k}{\varepsilon_k}\\&=\frac{m}{(2\pi)^3}\int[(g^{(0)}_1)^2+(g^{(0)}_2)^2]\frac{d^3k}{\varepsilon_k}=1\end{aligned} \tag{57}$$

with

$$\Pi^{\mu\nu}=\frac{1}{3}\sum_\lambda e^{\mu*}(p,\lambda)e^\nu(p,\lambda)=\frac{1}{3}\left(\frac{p^\mu p^\nu}{M^2}-g^{\mu\nu}\right). \tag{58}$$

The spin structures $S^{(0)}_{i\mu}$ are orthonormalized relative to the trace operation in Eq. (57) [cf. Eq. (40)],

$$\Pi^{\mu\nu}\mathrm{Tr}\{\bar{S}^{(0)}_{i\mu}(\hat{k}_2+m)S^{(0)}_{j\nu}(\hat{k}_1-m)\}=\delta_{ij}. \tag{59}$$

Note that $\bar{S}^{(0)}_{i\mu}=\gamma_0S^{(0)\dagger}_{i\mu}\gamma_0=S^{(0)}_{i\mu}$. Similar to Eq. (42) we get

$$\begin{aligned}&[4(\vec{k}^{\,2}+m^2)-M^2](\hat{k}_2+m)\phi^{(0)}_\mu(\hat{k}_1-m)\\&\quad=-\frac{m^2}{2\pi^3}\int\frac{g^2}{4m^2(Q^2+\mu^2)}(\hat{k}_2+m)O_2(\hat{k}'_2+m)\phi'^{(0)}_\mu\\&\qquad\times(\hat{k}'_1-m)\tilde{O}_1(\hat{k}_1-m)\frac{d^3k'}{\varepsilon_{k'}}.\end{aligned} \tag{60}$$

In order to obtain the system of equations for components $g^{(0)}_i$, we multiply Eq. (60) by $\Pi^{\mu\nu}$ and $S^{(0)}_{i\nu}$. Taking the trace and using the orthogonality condition (59) we obtain the system of equations

$$\begin{aligned}[4(\vec{k}^2+m^2)-M^2]g^{(0)}_i(\vec{k},\vec{n})&=-\frac{m^2}{2\pi^3}\int\sum_{j=1}^{2}K^{(0)}_{ij}(\vec{k},\vec{k}',\vec{n})g^{(0)}_j\\&\quad\times(\vec{k}',\vec{n})\frac{d^3k'}{\varepsilon_{k'}},\end{aligned} \tag{61}$$

which provides the mass of the $J=1, a=0$ state. They have the same form as Eq. (43), with kernels $K^{(0)}_{ij}$ given in terms of $\kappa^{(0)}_{ij}$ integrated over the azimuthal angle φ':

$$K^{(0)}_{ij}=\frac{1}{m^2\varepsilon_k\varepsilon_{k'}}\int_0^{2\pi}\frac{\kappa^{(0)}_{ij}}{Q^2+\mu^2}\frac{d\varphi'}{2\pi}. \tag{62}$$

For S, PS, and PV couplings they read

$$\kappa_{ij}^{(0)} = \frac{1}{4}\varepsilon_k\varepsilon_k'\Pi^{\mu\nu}\mathrm{Tr}[S_{i\mu}^{(0)}(\hat{k}_2+m)O_2(\hat{k}_2'+m)S_{j\nu}'^{(0)} \times(\hat{k}_1'-m)\tilde{O}_1(\hat{k}_1-m)], \quad (63)$$

where $S_{j\nu}'^{(0)}$ denotes Eq. (55) with primed arguments. For vector exchange

$$\kappa_{ij}^{(0)} = -\tfrac{1}{4}\varepsilon_k\varepsilon_k'\Pi^{\nu\mu}L_{\alpha\beta}\mathrm{Tr}[S_{i\nu}^{(0)}(\hat{k}_2+m)O_2^{\alpha}(\hat{k}_2'+m) \times S_{j\mu}'^{(0)}(\hat{k}_1'-m)O_1^{\beta}(\hat{k}_1-m)], \quad (64)$$

Tensors $L_{\alpha\beta}$ and $\Pi^{\nu\mu}$ are defined in Eqs. (14) and (58). The analytic expressions of $\kappa_{ij}^{(0)}$ for S, PS, PV, and V ($f_t=0$) exchanges are given in Appendix A.

B. $a=1$

It follows also from Eq. (30) that $\vec{\psi}^{(1)}$, the A^2 eigenfunction corresponding to $a=1$, is orthogonal to $\vec{n}$, i.e., satisfies $\vec{n}\cdot\vec{\psi}^{(1)}=0$. To fulfill this condition, it is convenient to introduce two vectors $(\hat{\vec{k}}_\perp, \vec{\sigma}_\perp)$ orthogonal to $\vec{n}$:

$$\hat{\vec{k}}_\perp = \frac{\hat{\vec{k}}-\cos\theta\vec{n}}{\sin\theta}, \quad \vec{\sigma}_\perp = \vec{\sigma}-(\vec{n}\cdot\vec{\sigma})\vec{n},$$

with $\hat{\vec{k}}=\vec{k}/k$ and $|\hat{\vec{k}}_\perp|=1$. Function $\vec{\psi}^{(1)}$ then obtains the decomposition, analogous to Eq. (52),

$$\vec{\psi}^{(1)}(\vec{k},\vec{n}) = g_1^{(1)}\frac{\sqrt{3}}{2}\vec{\sigma}_\perp + g_2^{(1)}\frac{\sqrt{3}}{2}[2\hat{\vec{k}}_\perp(\hat{\vec{k}}_\perp\cdot\vec{\sigma}_\perp)-\vec{\sigma}_\perp] + g_3^{(1)}\sqrt{\frac{3}{2}}\hat{\vec{k}}_\perp(\vec{\sigma}\cdot\vec{n}) + g_4^{(1)}\sqrt{\frac{3}{2}}i[\hat{\vec{k}}\times\vec{n}] \quad (65)$$

in terms of the four scalar amplitudes $g_i^{(1)}$. It can also be represented in the form of Eq. (51) by defining components $f_i^{(1)}$,

$$f_1^{(1)} = \sqrt{\frac{2}{3}}g_1^{(1)},$$

$$f_2^{(1)} = \frac{2}{\sqrt{3}\sin^2\theta}g_2^{(1)},$$

$$f_3^{(1)} = -\frac{1}{\sqrt{3}}g_1^{(1)} + \frac{(1+\cos^2\theta)}{\sqrt{3}\sin^2\theta}g_2^{(1)} - \frac{\sqrt{2}}{\sqrt{3}}\cot\theta g_3^{(1)},$$

$$f_4^{(1)} = -\frac{2\sqrt{3}\cos\theta}{3\sin^2\theta}g_2^{(1)} + \frac{1}{\sqrt{6}\sin\theta}g_3^{(1)},$$

$$f_5^{(1)} = \frac{1}{\sin\theta}g_4^{(1)},$$

$$f_6^{(1)} = -\frac{1}{\sqrt{2}\sin\theta}g_3^{(1)} \quad (66)$$

and in the four-dimensional form $\phi_\mu^{(1)}$ similar to Eq. (50),

$$\phi_\mu^{(1)} = g_1^{(1)}S_{1\mu}^{(1)} + g_2^{(1)}S_{2\mu}^{(1)} + g_3^{(1)}S_{3\mu}^{(1)} + g_4^{(1)}S_{4\mu}^{(1)}. \quad (67)$$

The four spin structures $S_{j\mu}^{(1)}$ are orthonormalized according to Eq. (59) and read

$$S_{i\mu}^{(1)} = \sum_j h_{ij}S_{j\mu}, \quad i=1,\ \ldots,4; j=1,\ \ldots,6, \quad (68)$$

with $S_{j\mu}$ defined in Eq. (48) and h_{ij} coefficients given in Appendix B. The normalization condition in terms of $\phi_\mu^{(1)}$ and $\vec{\psi}^{(1)}$ exactly coincides with Eq. (57). In terms of components $g_i^{(1)}$ it becomes

$$\frac{m}{(2\pi)^3}\int[(g_1^{(1)})^2+(g_2^{(1)})^2+(g_3^{(1)})^2+(g_4^{(1)})^2]\frac{d^3k}{\varepsilon_k}=1. \quad (69)$$

The system of equations for the scalar functions $g_i^{(1)}$ is obtained similar to Eq. (61) and reads

$$[4(\vec{k}^2+m^2)-M^2]g_i^{(1)}(\vec{k},\vec{n}) = -\frac{m^2}{2\pi^3}\int\sum_{j=1}^{4}K_{ij}^{(1)}(\vec{k},\vec{k}',\vec{n})g_j^{(1)}(\vec{k}',\vec{n})\frac{d^3k'}{\varepsilon_{k'}}. \quad (70)$$

It is the mass equation of the $J=1$, $a=1$ states. Kernels $K_{ij}^{(1)}$ are calculated in a way similar to Eq. (62). Corresponding $\kappa_{ij}^{(1)}$ are obtained with the replacement $S_{i\mu}^{(0)}\to S_{i\mu}^{(1)}$ in Eqs. (63) and (64). Their analytic expressions for S and PS exchanges are given in Appendix A.

C. Physical solution

The solutions $\vec{\psi}^{(a)}$ constructed in the preceding sections, although being exact eigenstates of the truncated Hamiltonian, are only auxiliary. As explained in Sec. III, the solution satisfying the angular condition (20) is given by superposition (31) of states with different a. The coefficients c_a of the superposition can be obtained by solving the angular condition in the truncated Fock space. We will show in what follows that they can alternatively be determined by imposing the independence of the wave function on the light-front vector $\vec{n}$ at $k=0$.

In order to do this, it is convenient to write down $\vec{\psi}^{(a)}$ in the form of Eq. (51) with the components $f_i^{(a)}$ given by Eqs. (53) and (66). Written in terms of f's, superposition (31) reads

$$f_i = c_0 f_i^{(0)} + c_1 f_i^{(1)}. \quad (71)$$

The condition that $\vec{\psi}(\vec{k}=0,\vec{n})$ does not depend on $\vec{n}$ becomes

$$\partial_\theta f_i(k=0,\theta)\equiv 0, \quad i=1,2; \quad (72)$$

$$f_j(k=0,\theta)\equiv 0, \quad j=3,4,5,6. \tag{73}$$

Let us show that there exist two coefficients c_a, normalized to $c_0^2+c_1^2=1$, satisfying the six equations above. They are determined by only the values at $k=0$ of the first components $g_1^{(a)}$.

To this aim, we consider the behavior of $f_i^{(a)}(k,z)$ in the $k\to 0$ limit. The components in front of structures involving the unit vector $\hat{k}$ are $f_{2,4,5,6}^{(a)}$. By construction, they must vanish at $k=0$, i.e., satisfy

$$f_{2,4,5,6}^{(a)}(k=0,\theta)\equiv 0, \quad a=0,1. \tag{74}$$

Concerning $a=0$ states, this condition is trivially satisfied by $f_{2,5}^{(0)}$ since from Eq. (53) they are identically zero, whereas $f_{4,6}^{(0)}$ will satisfy Eq. (74) if

$$g_1^{(0)}(k=0,\theta)=+b_0\cos\theta, \tag{75}$$

$$g_2^{(0)}(k=0,\theta)=-b_0\sin\theta,$$

b_0 being *a priori* an arbitrary function of θ which later on will be shown to be constant. The only components which are nonzero at $k=0$ are $f_{1,3}^{(0)}$. Inserting values (75) in Eq. (53) we find

$$f_1^{(0)}(0,\theta)=\frac{1}{\sqrt{3}}\cos\theta g_1^{(0)}(0,\theta)-\frac{1}{\sqrt{3}}\sin\theta g_2^{(0)}(0,\theta)=\frac{1}{\sqrt{3}}b_0,$$

$$f_3^{(0)}(0,\theta)=-\frac{\sqrt{2}}{\sqrt{3}\sin\theta}g_2^{(0)}(0,\theta)=\sqrt{\frac{2}{3}}b_0.$$

Concerning $a=1$ solutions, determined by four independent components $g_i^{(1)}$, we see from Eq. (66) that condition (74) implies $g_{2,3,4}^{(1)}(0,\theta)\equiv 0$. The only nonvanishing component at $k=0$ is thus $g_1^{(1)}$ and we will denote by b_1 its value:

$$g_1^{(1)}(0,\theta)=b_1. \tag{76}$$

By inserting this value in Eq. (66) we get

$$f_1^{(1)}(0,\theta)=\sqrt{\frac{2}{3}}g_1^{(1)}(0,\theta)=\sqrt{\frac{2}{3}}b_1,$$

$$f_3^{(1)}(0,\theta)=-\frac{1}{\sqrt{3}}g_1^{(1)}(0,\theta)+\frac{(1+\cos^2\theta)}{\sqrt{3}\sin^2\theta}g_2^{(1)}(0,\theta)$$
$$-\frac{\sqrt{2}}{\sqrt{3}}\cot\theta g_3^{(1)}(0,\theta)=-\frac{1}{\sqrt{3}}b_1.$$

Components $f_3^{(0)}$ and $f_3^{(1)}$ are the only $\vec{n}$-dependent structures which give nonzero contributions at $k=0$ in the corresponding wave functions $\vec{\psi}^{(0)}$ and $\vec{\psi}^{(1)}$. These contributions must cancel in the physical wave function $\vec{\psi}$, which gives the relation

$$f_3(0,\theta)=c_0 f_3^{(0)}(0,\theta)+c_1 f_3^{(1)}(0,\theta)=c_0\sqrt{\frac{2}{3}}b_0-c_1\frac{1}{\sqrt{3}}b_1=0.$$

This relation, together with the normalization condition $c_0^2+c_1^2=1$, allows us to determine the coefficients c_a of the superposition (31). They read

$$c_0=\frac{b_1}{\sqrt{2b_0^2+b_1^2}}, \qquad c_1=\frac{\sqrt{2}b_0}{\sqrt{2b_0^2+b_1^2}}. \tag{77}$$

We see from the above expressions that conditions (72) and (73) will be satisfied if and only if coefficients b_a are actually independent of θ.

It is worth noting that if the wave function $\vec{\psi}$ does not depend on $\vec{n}$, these coefficients become especially simple:

$$c_0=\sqrt{\frac{1}{3}}, \quad c_1=\sqrt{\frac{2}{3}}. \tag{78}$$

Indeed, from an $\vec{n}$-independent wave function $\vec{\psi}$ we can construct normalized $\vec{n}$-dependent states with definite a as follows:

$$\vec{\psi}^{(0)}(\vec{k},\vec{n})=\sqrt{3}\vec{n}[\vec{n}\cdot\vec{\psi}(\vec{k})],$$

$$\vec{\psi}^{(1)}(\vec{k},\vec{n})=\sqrt{\frac{3}{2}}\{\vec{\psi}(\vec{k})-\vec{n}[\vec{n}\cdot\vec{\psi}(\vec{k})]\}.$$

The initial function $\vec{\psi}(\vec{k})$ is reproduced by taking their superposition with coefficients (78). In the case of scalar constituents, we found [65] that coefficients c_a are very close (with the accuracy $\approx 1\%$) to values (78), despite the fact that the wave function strongly depended on $\vec{n}$ and the split between M_0 and M_1 masses was large.

Let us finally summarize the procedure followed to construct the physical wave function. The solution of the mass equations (61) and (70) provides the mass squared M_a^2 and the components $g_{1,2}^{(0)}$ and $g_{1-4}^{(1)}$ of the A^2 eigenstates. The nonzero values of the first components $g_1^{(a)}$ at $k=0$ determine—by means of Eqs. (75) and (76)—the coefficients b_a. These are inserted in Eq. (77) to provide c_a, coefficients of the linear combination determining the physical mass M^2 from Eq. (32) and the components (71) of wave function (51). Components $f_i^{(a)}$ of this superposition are related to $g_j^{(a)}$ by Eqs. (53) and (66), respectively.

VI. NONRELATIVISTIC LIMIT

In the following sections the LFD results will be compared to the corresponding nonrelativistic limits. By this we mean the zero-order terms in the $1/m$ expansion of the LFD equations and kernels. This section is devoted to precisely describing how this limit is obtained in the different OBE kernels, having in mind in each case: (i) what are the LFD wave function components that should be retained and (ii) what kind of equations will they satisfy.

In order to have some insight in the weak coupling limit, but also as a test for numerical calculations, it is often useful

to consider the LFD solutions as a perturbation of the nonrelativistic wave functions. This approximation was used in Refs. [58,59] to calculate the *NN S*-wave function and deuteron electromagnetic form factors [61]. We will also present in what follows how these first-order relativistic corrections can be obtained in the different mass equations (38) and (61) we consider.

A. $J=0$ states

For the scalar exchange the leading contribution in the kernel matrix is, according to Eq. (A4),

$$K_{11} = -\frac{4\pi\alpha}{(\vec{k}-\vec{k}')^2+\mu^2} \equiv V_S(\vec{k}-\vec{k}'). \tag{79}$$

Corrections to this kernel are of the $1/m^2$ order both in diagonal and nondiagonal terms. It follows that the $J=0$ wave function (38) contains in the nonrelativistic limit the f_1 component only, which is furthermore independent of θ. Introducing nonrelativistic kinematics, i.e., $4(\vec{k}^2+m^2) - M^2 \approx 4(k^2+mB)$, where $B=2m-M \ll m$ is the binding energy, the equation for $f_1 \equiv f_{NR}$ component becomes

$$(k^2+mB) f_{NR}(k) = -m \int V_S(\vec{k}-\vec{k}') f_{NR}(k') \frac{d^3k'}{(2\pi)^3} \tag{80}$$

with kernel (79). This is the Schrödinger equation with the Yukawa potential $V_S(r) = -\alpha \exp(-\mu r)/r$.

For vector exchange we obtain the same equation (80) with a kernel differing from Eq. (79) by a global sign. This corresponds to the repulsion between two fermions (e^-e^-, for instance).

We see that for the scalar and vector couplings, the nonrelativistic limit of LFD equations coincides with the one-component Schrodinger equation.

For pseudoscalar and pseudovector exchanges the leading diagonal kernels are of the $1/m^2$ order, whereas the nondiagonal ones are of $1/m^3$. Thus, for these couplings the nonrelativistic limit does not exist. In the leading order and since the K_{22} kernel is repulsive, only the f_1 component remains. The corrections due to f_2 are expected to be larger than for scalar and vector cases. Component f_1 satisfies at this order the Schrodinger equation (80) with a kernel proportional to $1/m^2$:

$$V_{PS}(\vec{k}-\vec{k}') = \frac{\pi\alpha}{(\vec{k}-\vec{k}')^2+\mu^2} \frac{(\vec{k}-\vec{k}')^2}{m^2}$$

$$= \frac{\pi\alpha}{m^2}\left[1 - \frac{\mu^2}{(\vec{k}-\vec{k}')^2+\mu^2}\right]. \tag{81}$$

In coordinate space it corresponds to

$$V_{PS}(\vec{r}) = \frac{\pi\alpha}{m^2}\left[\delta^{(3)}(\vec{r}) - \frac{\mu^2}{4\pi}\frac{\exp(-\mu r)}{r}\right]. \tag{82}$$

For these couplings the leading term is of the same order as the relativistic correction in the scalar and vector cases. We will see that a similar situation takes place for the $J=1$ state. This fact makes an important difference between the couplings. Pseudoscalar and pseudovector exchanges appear always as being relativistic corrections.

We would like to remark from the above results that in the nonrelativistic limit the $\vec{n}$-dependent terms in the LFD wave function (38) and kernels disappear.

For models involving the sum of all exchanges (such as for the OBE *NN* interaction) the nonrelativistic limit is determined only by the S and V exchanges. First-order corrections can be obtained by inserting the nonrelativistic component $f_1 = f_{NR}$ into the right-hand side of Eq. (43).

$$[4(\vec{k}^2+m^2) - M^2] f_i(k,\theta) = -\frac{m^2}{2\pi^3}\int K_{i1}(k,\theta;k',\theta') f_{NR}(k') \frac{d^3k'}{\varepsilon_{k'}}. \tag{83}$$

They generate a perturbative solution for the two components, which incorporates the first-order relativistic effects. This approach was followed in Ref. [59] to obtain the $^1S_0$ *NN* scattering wave function.

B. $J=1$ states

For $J=1$ states, components $g_i^{(a)}$ obtained by solving the mass equations differ from those appearing in the wave function f_i. Our first step is to determine the form of $g_i^{(a)}$ in the case of a nonrelativistic wave function. The nonrelativistic wave function components do not depend on $\vec{n}$ and, according to Eq. (78), are given by

$$f_i = \frac{1}{\sqrt{3}} f_i^{(0)} + \sqrt{\frac{2}{3}} f_i^{(1)}. \tag{84}$$

Substituting Eq. (84) into Eqs. (53) and (66) we obtain a relation between f_i and $g_j^{(a)}$ components. These equations are solved relative to $g_j^{(a)}$ and the result, expressed through f_i, reads

$$g_1^{(0)} = f_1 \cos\theta + f_2\sqrt{2}\cos\theta + f_3\sqrt{2}\cos\theta + f_4\frac{7+\cos 2\theta}{2\sqrt{2}} + f_6\sqrt{\frac{3}{2}}\sin^2\theta,$$

$$g_2^{(0)} = -f_1 \sin\theta + f_2\frac{1}{\sqrt{2}}\sin\theta - f_3\sqrt{2}\sin\theta - f_4\frac{1}{2\sqrt{2}}\sin 2\theta + f_6\sqrt{\frac{3}{8}}\sin 2\theta,$$

$$g_1^{(1)} = f_1 - f_2\frac{1+3\cos 2\theta}{4\sqrt{2}} - f_3\frac{1}{\sqrt{2}} - f_4\sqrt{2}\cos\theta,$$

$$g_2^{(1)} = f_2\frac{3}{2\sqrt{2}}\sin^2\theta,$$

$$g_3^{(1)} = f_2 \frac{3}{4} \sin 2\theta + f_4 \frac{3}{2} \sin \theta - f_6 \frac{\sqrt{3}}{2} \sin \theta,$$

$$g_4^{(1)} = f_5 \sqrt{\frac{3}{2}} \sin \theta. \tag{85}$$

As previously discussed, in the nonrelativistic limit there are no $\vec{n}$-dependent terms in the LFD wave function (51) and only f_1 and f_2 components among the six f_i survive. We have shown in Ref. [58] that one actually has $f_1 \approx u_S$, $f_2 \approx -u_D$, $f_{3-6} \approx 0$, where u_S and u_D are, respectively, the usual S- and D-wave nonrelativistic components. Inserting these expressions in Eq. (85) we obtain the form of the nonrelativistic functions g:

$$g_1^{(0)} = (u_S - \sqrt{2} u_D) \cos \theta,$$

$$g_2^{(0)} = -\left(u_S + \frac{1}{\sqrt{2}} u_D \right) \sin \theta,$$

$$g_1^{(1)} = u_S + \frac{1}{4\sqrt{2}} (1 + 3 \cos 2\theta) u_D,$$

$$g_2^{(1)} = -\frac{3}{2\sqrt{2}} \sin^2 \theta u_D,$$

$$g_3^{(1)} = -\frac{3}{4} \sin 2\theta \, u_D,$$

$$g_4^{(1)} = 0. \tag{86}$$

We see here that the θ dependence of the auxiliary components $g_i^{(a)}$ remains even in the nonrelativistic limit. It will disappear only in the linear combination, giving the physical components $f_{1,2}$.

Let us first consider the scalar exchange. The mass equation for $a=0$ eigenstate (61) and the scalar kernels (A1) become in the leading order $(1/m)^0$,

$$C(k) g_1^{(0)}(k, \theta) = -4\alpha\pi \cos \theta \int [g_1^{(0)}(k', \theta') \cos \theta' - g_2^{(0)}(k', \theta') \sin \theta'] \{\cdots\} \frac{d^3k'}{\varepsilon_{k'}},$$

$$C(k) g_2^{(0)}(k, \theta) = +4\alpha\pi \sin \theta \int [g_1^{(0)}(k', \theta') \cos \theta' - g_2^{(0)}(k', \theta') \sin \theta'] \{\cdots\} \frac{d^3k'}{\varepsilon_{k'}}. \tag{87}$$

For shortness we denote by $C(k)$ the kinematical part and by $\{\cdots\}$ the kernel contributions which are common to all couplings and states.

$$\{\cdots\} = \frac{1}{m^2 \varepsilon_k \varepsilon_{k'}} \frac{1}{Q^2 + \mu^2}.$$

These factors contain $1/m$ and $1/m^2$ terms but we do not write them explicitly and analyze only the kernel contributions resulting from κ_{ij}.

Since the integrals on the right-hand sides of Eq. (87) are the same, its solution has the form

$$g_1^{(0)}(k, \theta) = +g^{(0)}(k) \cos \theta,$$

$$g_2^{(0)}(k, \theta) = -g^{(0)}(k) \sin \theta, \tag{88}$$

with $g^{(0)}$ an unknown function to determine. Substituting Eq. (88) into Eq. (87) we find the equation for $g^{(0)}$:

$$C(k) g^{(0)}(k) = -4\alpha\pi \int g^{(0)}(k') \{\cdots\} \frac{d^3k'}{\varepsilon_{k'}}. \tag{89}$$

For $a=1$ state, we found in a similar way that only $g_1^{(1)}$ survives and satisfies to the same $(1/m)^0$ order the equation

$$C(k) g_1^{(1)}(k, \theta) = -4\alpha\pi \int g_1^{(1)}(k', \theta') \{\cdots\} \frac{d^3k'}{\varepsilon_{k'}}. \tag{90}$$

It coincides with Eq. (89) for $a=0$ and, hence, provides the same mass. We see in this way that, in the leading order, $a=0$ and $a=1$ states are degenerate. The coefficients c_a of superposition (71) are calculated in terms of b_a given by Eqs. (75) and (76). Since in the leading order $g_1^{(0)}$ and $g_1^{(1)}$ equal $g^{(0)}$, one has $b_0 = b_1 = g^{(0)}(0)$ and, from Eq. (77), values (78).

In the next-to-leading order—$1/m^2$—we get for $a=0$

$$C(k) g_1^{(0)} = \alpha\pi \frac{1}{m^2} \int [2 g'^{(0)}_1 kk' - 3(k^2 + k'^2) \times \cos \theta (g'^{(0)}_1 \cos \theta' - g'^{(0)}_1 \sin \theta')] \{\cdots\} \frac{d^3k'}{\varepsilon_{k'}},$$

$$C(k) g_2^{(0)} = \alpha\pi \sin \theta \frac{1}{m^2} \int 3(k^2 + k'^2)(g'^{(0)}_1 \cos \theta' - g'^{(0)}_1 \sin \theta') \{\cdots\} \frac{d^3k'}{\varepsilon_{k'}} \tag{91}$$

and for $a=1$,

$$C(k) g_1^{(1)} = -\alpha\pi \frac{1}{m^2} \int [3(k^2 + k'^2) g'^{(1)}_1 + kk' \cos \theta (-2 g'^{(1)}_1 \times \cos \theta' + \sqrt{2} g'^{(1)}_3 \sin \theta')] \{\cdots\} \frac{d^3k'}{\varepsilon_{k'}},$$

$$C(k)g_3^{(1)} = -\alpha\pi \sin\theta \frac{1}{m^2}\int kk'(\sqrt{2}g'^{(1)}_1 \cos\theta' - g'^{(1)}_3 \sin\theta')\{\cdots\}\frac{d^3k'}{\varepsilon_{k'}}. \quad (92)$$

These systems of equations—Eqs. (91) and (92)—are already different and the masses of the two eigenstates are split.

For vector exchange, the situation is quite similar. The equations in the leading order $(1/m)^0$ differ from Eqs. (87) and (90) only by a global sign on their right-hand sides. Thus for these two couplings, as it was the case for $J=0$, the leading order is $(1/m)^0$.

For pseudoscalar exchange, the leading contribution in the kernel has order $1/m^2$. Indeed, from the analytic expressions given in Eqs. (A2), we found for the $a=0$ state

$$g_1^{(0)} = \alpha\pi \cos\theta \frac{1}{m^2}\int k'^2(g_1^{(0)}\cos\theta' + g_2^{(0)}\sin\theta')\{\cdots\}\frac{d^3k'}{\varepsilon_{k'}},$$

$$g_2^{(0)} = -\alpha\pi \sin\theta \frac{1}{m^2}\int k'^2(g_1^{(0)}\cos\theta' + g_2^{(0)}\sin\theta')\{\cdots\}\frac{d^3k'}{\varepsilon_{k'}}. \quad (93)$$

Like for the scalar coupling, the solution of Eqs. (93) has the form (88) with $g^{(0)}$ satisfying the equation

$$g^{(0)} = \alpha\pi \frac{1}{m^2}\int k'^2(\cos^2\theta' - \sin^2\theta')g^{(0)}\{\cdots\}\frac{d^3k'}{\varepsilon_{k'}}. \quad (94)$$

For $a=1$ the leading order equation reads

$$g_1^{(1)} = -\alpha\pi \frac{1}{m^2}\int k'^2 \cos^2\theta' g_1^{(1)}\{\cdots\}\frac{d^3k'}{\varepsilon_{k'}}, \quad (95)$$

which is now different from Eq. (94). The masses M_0 and M_1 calculated with pseudoscalar exchange are therefore always different. Their difference remains even in systems having small binding energies or when the large momentum contributions are removed using small cutoff parameter Λ in form factors (18).

The pseudovector exchange kernel differs from the pseudoscalar one by the replacement $\gamma_5 \to \gamma_5 - \hat{\omega}\gamma_5 \pi/2m$ or by $\gamma_5 \to \gamma_5 + \hat{\omega}\gamma_5\tau'/2m$ [see Eq. (4.18) in Ref. [57]]. Thus there is an extra term proportional to $\hat{\omega}\gamma_5\tau'/2m \propto (k'^2 + m|B|)/m^2$ which does not contain $(1/m)^0$ terms. The situation is therefore the same as for the pseudoscalar case.

To summarize, we have shown analytically that in the nonrelativistic limit for scalar and vector exchanges, the energies $B(a=0)$ and $B(a=1)$ coincide with each other and the coefficients c_0 and c_1 tend to $\sqrt{\frac{1}{3}}$ and $\sqrt{\frac{2}{3}}$, respectively. On the contrary, for pseudoscalar and pseudovector couplings this is not the case. In this sense, for the pseudoscalar and pseudovector exchanges, the nonrelativistic limit does not exist. If the kernel is the sum of all the exchanges, such as the *NN* kernel, the situation is the same as for the scalar and vector exchanges, since in the nonrelativistic limit the $(1/m)^0$ order dominates, resulting from these exchanges. The existence of the deuteron, for example, as a nonrelativistic system (with a reasonable accuracy) is due to the contribution of the scalar and vector exchanges in the *NN* interaction.

Perturbative solutions are obtained by substituting the zero-order functions (86) into the right-hand sides of LFD equations (61) and (70). If the *D* wave is neglected, the six perturbative components are given in terms of the only nonrelativistic wave function u_S simply by

$$[4(\vec{k}^2 + m^2) - M^2]g_i^{(0)}(\vec{k},\vec{n}) = -\frac{m^2}{2\pi^3}\int (K_{i1}^{(0)}\cos\theta' - K_{i2}^{(0)}\sin\theta')u_S(k')\frac{d^3k'}{\varepsilon_{k'}}, \quad (96)$$

$$[4(\vec{k}^2 + m^2) - M^2]g_i^{(1)}(\vec{k},\vec{n}) = -\frac{m^2}{2\pi^3}\int K_{i1}^{(1)}u_S(k')\frac{d^3k'}{\varepsilon_{k'}}. \quad (97)$$

We would like to mention here that one appreciable advantage of the LFD formalism with respect to other relativistic approaches is the clear link it has with the nonrelativistic dynamics. This is because on one hand LFD wave functions have the same physical meaning of probability amplitudes, while on the other hand their components f_i split into two families: those which in the nonrelativistic limits become negligible and those which tend to the usual nonrelativistic wave functions.

The following sections are devoted to showing the numerical solutions obtained with differents couplings. Their very different behavior requires to be treated separately.

VII. RESULTS FOR SCALAR COUPLING

Our first results concerning the Yukawa model have been reported in Refs. [68,69]. The main interest in these papers concerned the stability of the $J=0,1$ solutions with respect to the cutoff, i.e., the possibility of getting stable results without any vertex form factor. We showed in particular that $J=0^+$ states were stable for coupling constant smaller than some critical value $\alpha \leqslant \alpha_c \simeq 3.72$ and unstable above. On the contrary, the $J=1^+$ states were found to be unstable for any value of the coupling constant and both projections $a=0,1$. This instability manifests in the logarithmic decrease of $M^2(k_{max})$ for a given value of α—or equivalently of $\alpha(k_{max})$ for a given value of M—and imposes the use of form factors.

We first consider the $J=0^+$ state. Its wave function is determined by two components f_i. Although the use of vertex form factors (FF) is not required [68], we would like to note that the convergence as a function of k_{max} is very slow. Unless otherwise specified the results that follow correspond to $\mu=0.15$.

For a weakly bound system ($B=0.001$), the coupling constant found by solving LFD equations is $\alpha_{Yuk}=0.331$, whereas the nonrelativistic (NR) value is $\alpha_{NR}=0.323$. By the latter we understand the results obtained by inserting into the

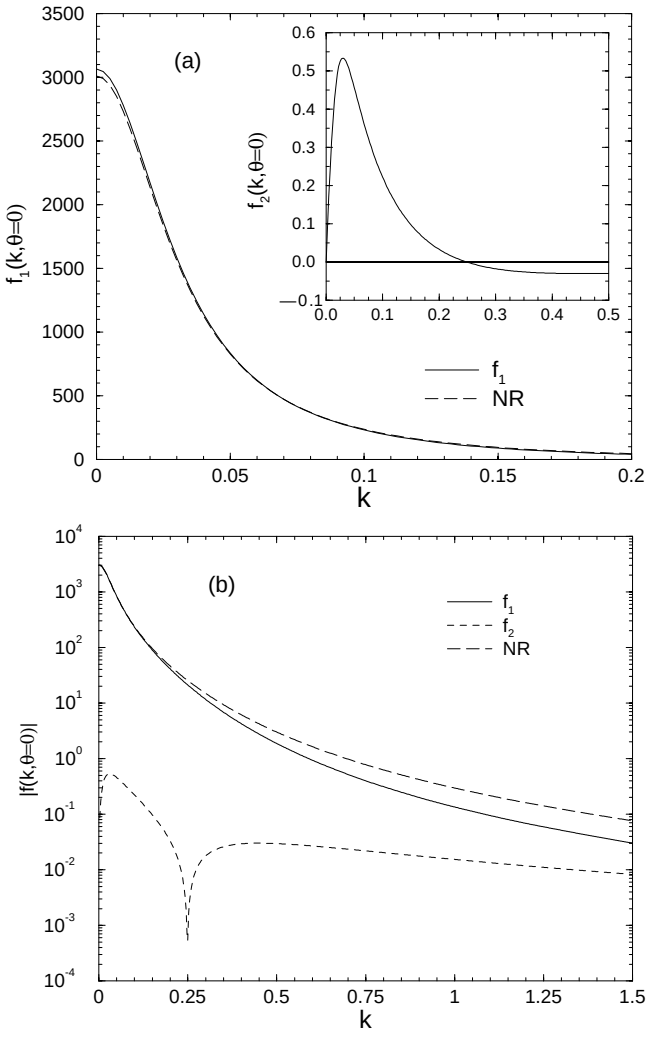

FIG. 4. LFD wave function components f_i for scalar coupling (B=0.001, μ=0.15) in (a) linear and (b) logarithmic scale compared with the nonrelativistic solutions.

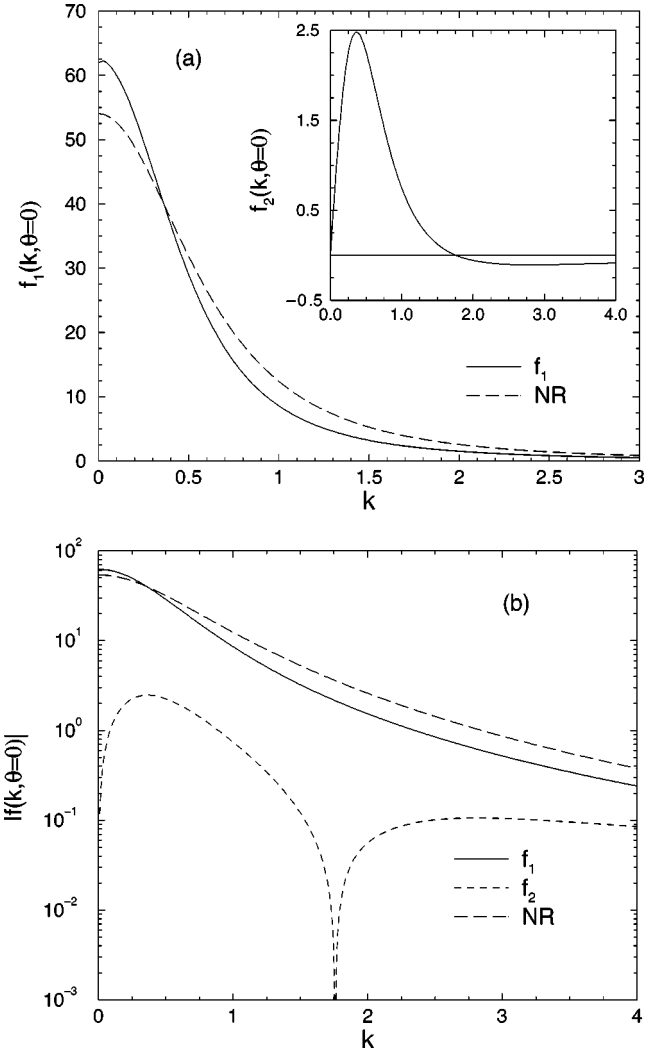

FIG. 5. LFD wave function components f_i for scalar coupling (B=0.5, μ=0.15) in (a) linear and (b) logarithmic scales compared with the nonrelativistic solutions.

Schrodinger equation (80) the static potential (79) resulting from the leading order approximation, as has been discussed in Sec. VI. As in the Wick-Cutkosky (WC) model—scalar particles interacting by scalar exchange—relativistic effects are repulsive [64]. They account for only a 3% difference in the coupling constants whereas in WC they are sizably bigger (α_{WC}=0.364).

Corresponding wave functions are displayed in Figs. 4(a) and 4(b). One can see that component f_1 dominates over f_2 in all the interesting momentum range and that f_2 has a zero at $k\approx 0.25$. One also notices in Fig. 4(b) that f_1 is very close to the NR wave function in the small momentum but it sensibly departs with increasing k; for $k\sim 1.5$ the differences represent more than one order of magnitude in the probability densities. The coupling between the two relativistic amplitudes has a very small (0.1%) attractive effect on the binding energy.

In the strong binding limit (B=0.5), the situation is quite similar with enhanced relativistic effects on binding energies and wave functions. One has α_{Yuk}=2.44 for α_{NR}=1.71 and the differences in the wave functions—displayed in Figs. 5(a) and 5(b)—are already visible at k=0 momentum (Fig. 5). One can see however in Fig. 5(b) that—even for deeply bound systems—f_1 component still dominates over f_2.

It is of some interest to compare the LFD results for Yukawa (two-fermion) and WC (two-scalar) models with the NR results. We have displayed in Fig. 6 the corresponding coupling constants for different values of the binding energy. One can see that the Yukawa results (α_{Yuk}) are systematically closer to the nonrelativistic values than α_{WC} are, as if the fermionic character of the constituents generates closer binding energies to the NR ones but larger differences in the high momentum components of the wave function, due to the different asymptotic of interaction kernels.

Though not necessary to get stable solutions, form factors have been widely used in most of the previous OBEP calculations performed in momentum space [60]. It is thus interesting to estimate their influence in the predictions. To this aim we have considered the vertex form factors used in the Bonn model (18) with, for the scalar coupling, n=1 and Λ =2.0. Their effects are found to be repulsive. For B=0.001

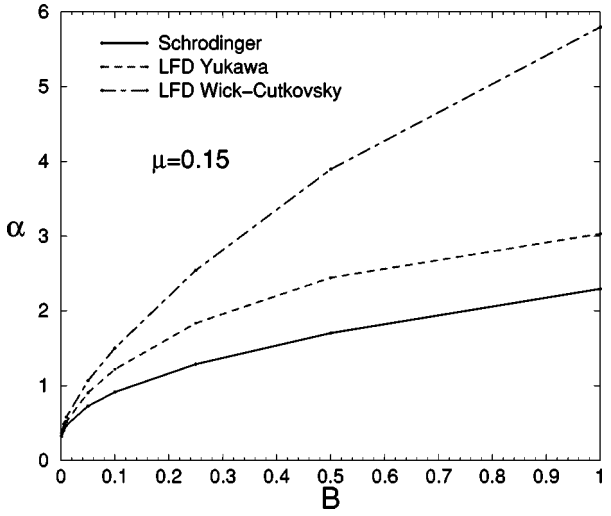

FIG. 6. Comparison of $B(\alpha)$ between the Yukawa (dashed line) and Wick-Cutkosky (dot dashed lines) models in LFD and nonrelativistic (solid line) results in $J=0^+$ state.

they remain relatively small ($\alpha_{Yuk}=0.376$ instead of $\alpha_{Yuk}0.331$) but for $B=0.5$ the differences reach already a factor 2 ($\alpha_{Yuk}=5.32$ instead of $\alpha_{Yuk}=2.44$). It is worth emphasizing that, whatever will be the degree of refinement in the dynamics, the results of a relativistic calculation will be strongly influenced by this phenomenological and not well controlled trick.

The system of equations for determining the $J=1^+, a=0$ ($g^{(a=0)}_{i=1,2}$) and $a=1$ ($g^{(a=1)}_{i=1,2,3,4}$) solutions are both unstable and require cutoff regularization [46,68]. This can be seen in Fig. 7 where the $\alpha(k_{max})$ variation for $a=0$ and $a=1$ cases displays a logarithmic dependence. One can also see in this figure the nondegeneracy of both states due to the Fock-space truncation discussed in Sec. III. We remark however that if the binding energies—or equivalently coupling constants—of

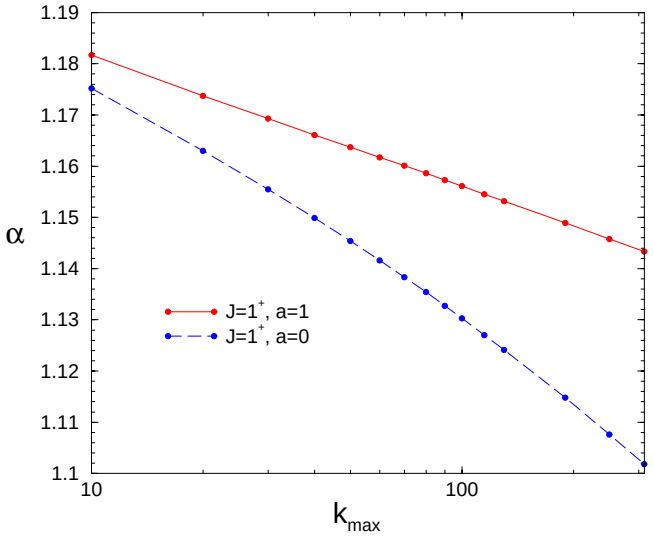

FIG. 7. Logarithmic dependence of the coupling constant as a function of cutoff for the $J=1^+$ $a=0$ and $a=1$ states. Calculations correspond to $B=0.05$ and $\mu=0.25$.

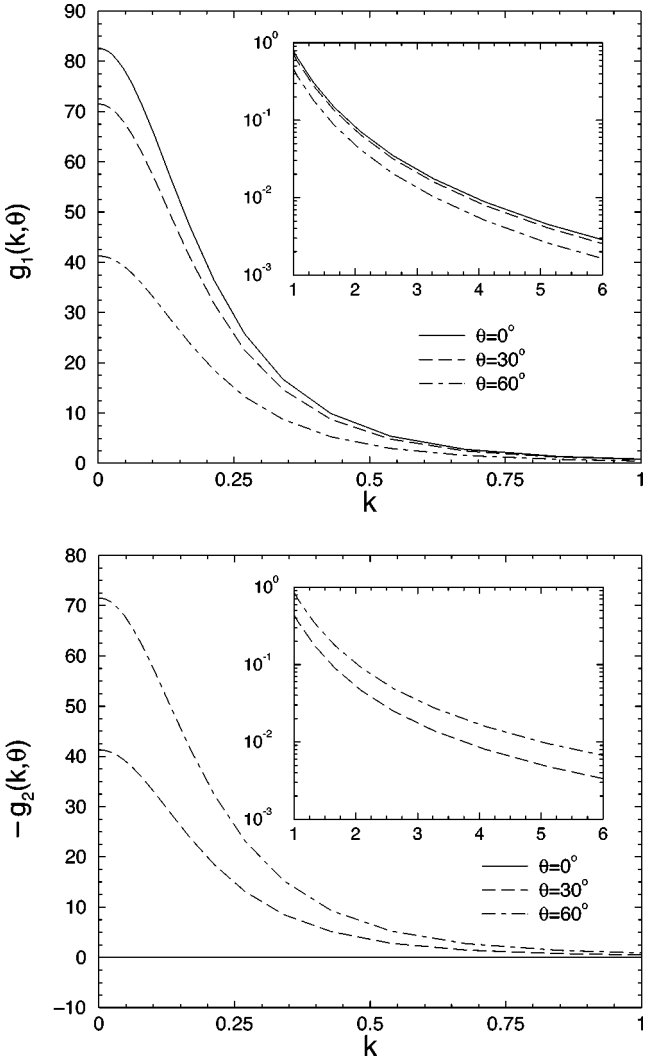

FIG. 8. $g^{a=0}_{i=1,2}$ solutions for scalar coupling with $\alpha=1.18$, $\mu=0.25$ and sharp cutoff at $k_{max}=10$. The binding energy is $B=0.0506$.

states with different projections a are not equal, they are almost degenerated in a wide range of k_{max} values. For instance, at $k_{max}=10$ one has $\alpha_{a=0}=1.17$ and $\alpha_{a=1}=1.18$, while at $k_{max}=90$ one has $\alpha_{a=0}=1.14$ and $\alpha_{a=1}=1.16$. These weak splittings of less than 1% for a noticeably bound system ($B=0.05$) are rather surprising in view of the results obtained in the purely scalar WC case [65,66], in which the difference in coupling constants for the same binding energy is 20%, which corresponds to $\Delta B \approx B$.

The $g^{(a)}_i$ solutions for $a=0$ and $a=1$ states are, respectively, represented in Figs. 8 and 9 for several values of θ. They were obtained with a coupling constant $\alpha_s=1.18$ and a sharp cutoff at $k_{max}=10$. We remark that with the conventions used $g^{(0)}_2(k,0)=0$ and one has $g^{(0)}_1(0,0)=-g^{(0)}_2(0,90°)$, as expected from Eqs. (75). In addition, $g^{(0)}_1(0,0)=-g^{(0)}_2(0,90°) \approx g^{(1)}_1(0,\theta)$, as expected from Eq. (76) and from the fact that coefficient c_i, defined in (77), are very close to values (78). Corresponding binding energies are $B_{a=0}=0.0506$ and

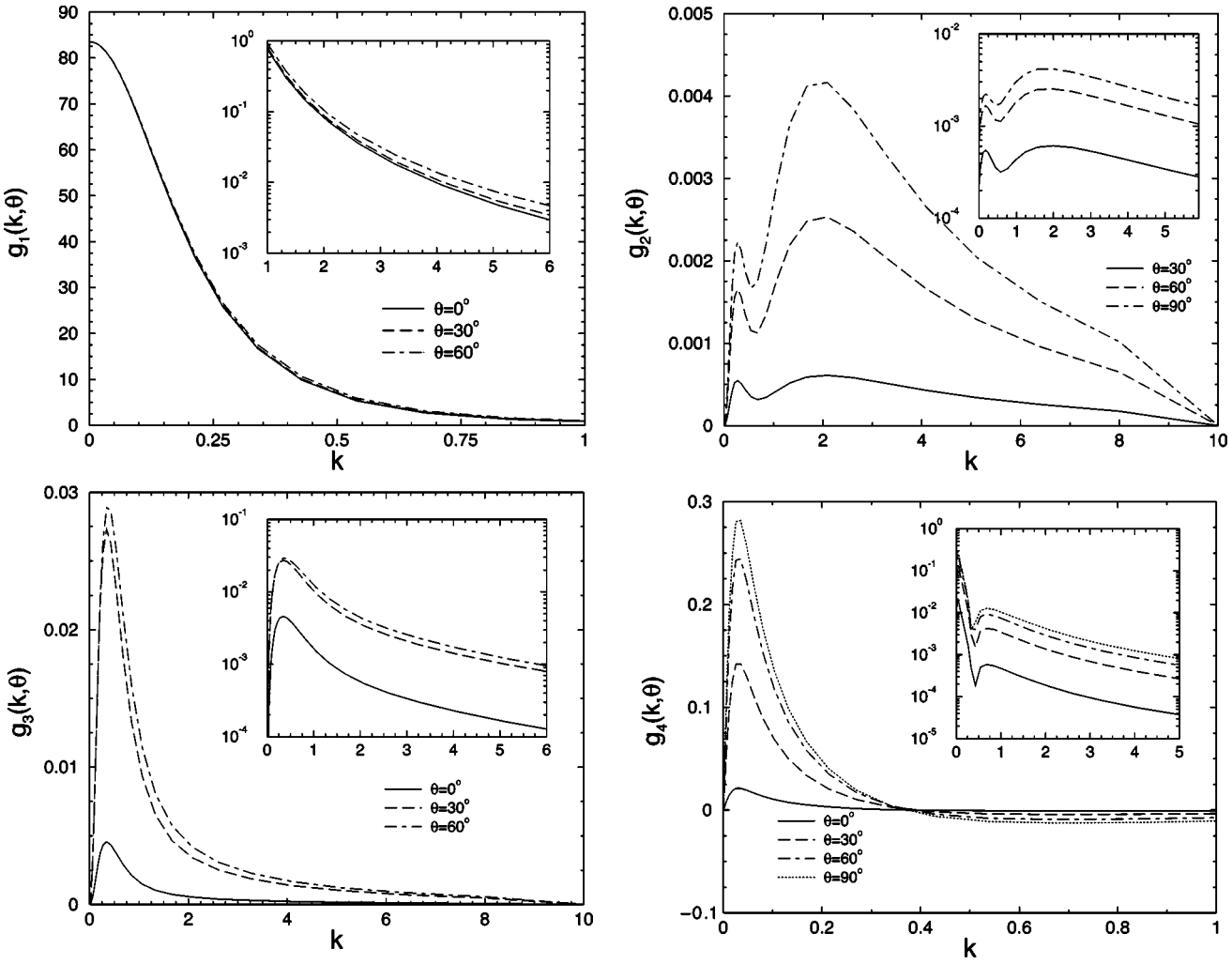

FIG. 9. $g^{a=1}_{i=1,\ldots,4}$ solutions for scalar coupling with α=1.18, μ=0.25, and sharp cutoff at k_{max}=10. The corresponding binding energy is B=0.0498.

$B_{a=1}$=0.0498, values which are 1% close to each other. The splitting of the binding energies is an increasing function of the coupling constant. Figure 10 shows the calculated $B_a(\alpha)$ dependence for both J=1 eigenstates. For α_s=0.55 the values are, respectively, $B_{a=0}=9.7\times10^{-3}$ and $B_{a=1}=9.6\times10^{-3}$ whereas for α_s=2.87, $B_{a=0}$=0.523 and $B_{a=1}$=0.467. The non-degeneracy remains reasonably small even for strongly bound systems.

The six components f_i of the $J=1^+$ physical wave function are determined by a linear combination (71) of functions $f_i^{(a)}$, which in their turn are expressed in terms of $g_i^{(a)}$ by Eqs. (53) and (66). Remember that coefficients c_a of this linear combination are computed from components $g_1^{(a=0,1)}$ only. For the solutions presented in Figs. 8 and 9 they are found to be c_0 =0.582 and c_1=0.813 and the corresponding energy is B =0.0501. Note that these values are very close to those obtained in the case of $\vec{n}$-independent interactions (78): c_0 $=1/\sqrt{3}=0.577$ and $c_1=\sqrt{2/3}=0.816$. They become even closer to these values for smaller binding energies and they smoothly depart for strongly bound systems. For a state with

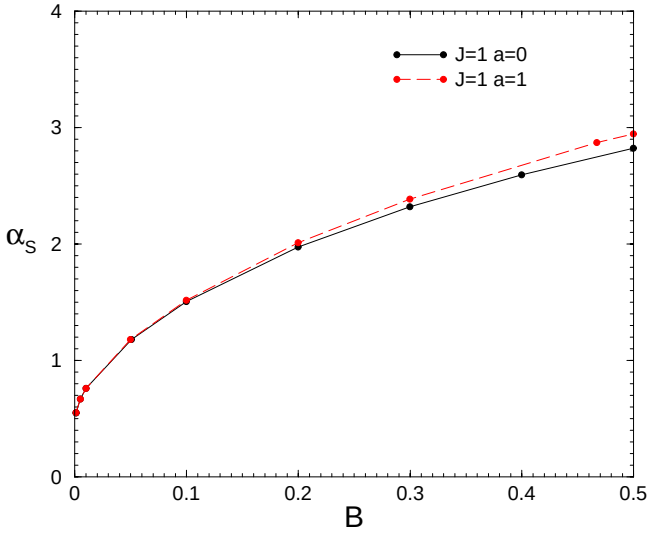

FIG. 10. Splitting of the J=1 solutions for the scalar coupling. Results correspond to μ=0.25 and sharp cutoff at k_{max}=10.

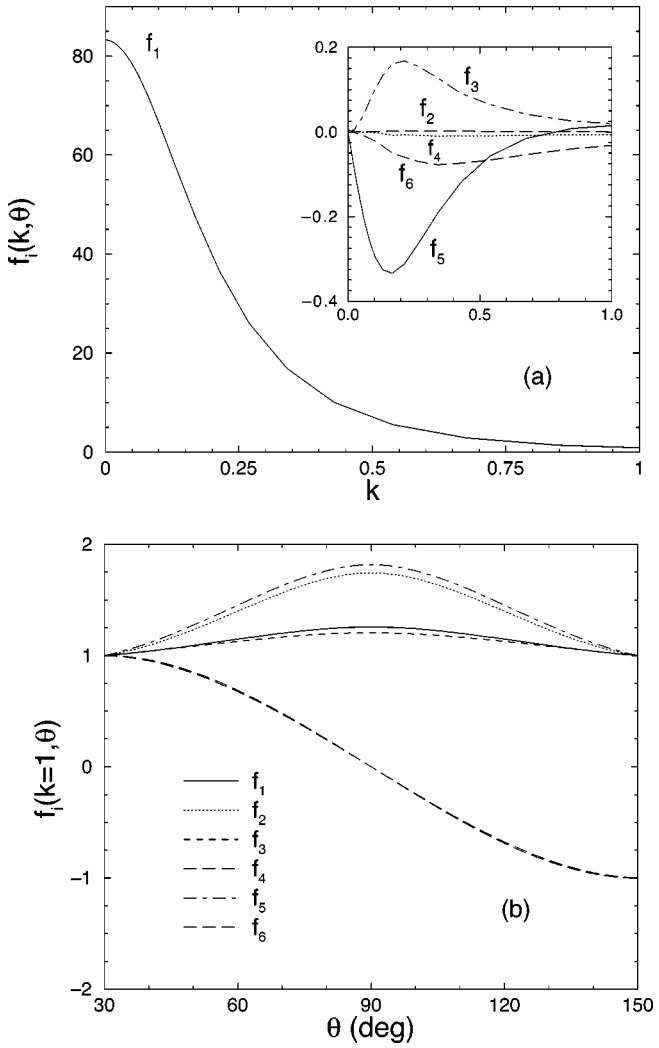

FIG. 11. Wave function components f_i of the physical solutions (a) as a function of k at $\theta=30°$ and (b) their θ dependence at fixed $k=1$ value. Calculations are for the scalar coupling with $\alpha=1.18$, $\mu=0.25$, and sharp cutoff $k_{max}=10$. Binding energy is $B=0.0501$.

$B\approx 0.5$ and the same sharp cutoff $k_{max}=10$ one has, for instance, $c_0=0.610$ and $c_0=0.793$. Components f_i thus obtained are displayed in Fig. 11 for $\theta=30°$ in linear (a) and logarithmic (b) scales. One can see that component f_1 dominates over the remaining five in the entire momentum range. Among the components of relativistic origin there is not a clear dominance. Notice the very small value of the f_2 component, corresponding to the tensor D wave, which would be absent in a nonrelativistic approach. These components have a definite parity in variable cos θ, $f_{1,2,3,5}$ being even and $f_{4,6}$ odd, as shown in Fig. 11(b) for a fixed value $k=1$.

VIII. RESULTS FOR PSEUDOSCALAR COUPLING

For pseudoscalar coupling, the stability analysis was performed using the same methods as for the scalar one [72,71] and it presents some peculiarities.

Equations for $J=0^+$ states are found to be stable without any regularization. The asymptotic behavior of the pseudoscalar kernel is the same as the scalar one; it has a repulsive

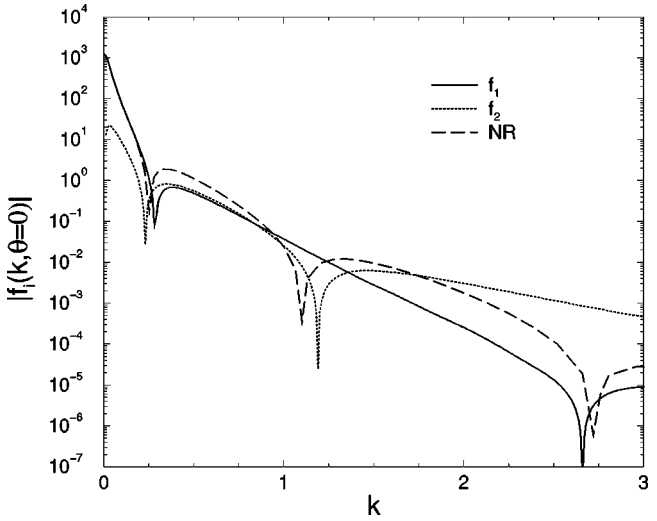

FIG. 12. Wave function components (in logarithmic scale) for $J=0^+$ state with $B=0.001$, $\mu=0.15$ obtained with pseudoscalar coupling and form factor $\Lambda=1.3$.

character which does not generate instability. The results lead to a quasidegeneracy of the coupling constants for binding energies which vary over all the physical range $[0, 2m]$. One gets, for instance, $\alpha=55.4$ for $B=0.001$ whereas $\alpha=58.5$ for a binding energy 500 times larger, $B=0.5$, showing an extreme sensibility of this model to small variations of the coupling constant. The origin of this behavior was found to lie in the second-channel equation (κ_{22}) and has been understood analytically [71] with a simple model. The use of form factors—though not required for the convergence of solutions—is necessary if one wishes to eliminate this unusual $\alpha(B)$ dependence. Calculations have thus been performed using form factors (18) with $n=1$ and $\Lambda=1.3$ as in the Bonn model.

In the weak binding limit ($B=0.001$) one has $\alpha_{LFD}=190$ and $\alpha_{NR}=166$, a repulsive effect much stronger (15%) than in the scalar coupling. Corresponding wave functions are shown in Fig. 12. One can see that the component of relativistic origin $f_2\approx f_1$ at $k\sim 0.3$ and dominates above $k=1$. A similar result was found in the $np\ ^1S_0$ scattering wave function calculated perturbatively with all the OBEP kernel in Ref. [59]. Contrary to the Yukawa model, the role of relativistic components is crucial already for such a loosely bound system. The coupling between components is also very important: by switching off the nondiagonal kernels $K_{12}=K_{21}=0$ the coupling constant moves from $\alpha_{LFD}=190$ to $\alpha_{LFD}=251$. It has thus an attractive effect which tends to minimize the difference between LFD and NR results. The comparison between f_1 and the nonrelativistic solution f_{NR} shows a very good agreement in small k. When k increases, large differences appear and f_{NR} even has an additional zero at $k=1.1$.

It is worth noting the dramatic influence of the form factor in all these calculations. One has, for instance, $\alpha_{LFD}=103$ for $\Lambda=5$ and $\alpha_{LFD}=1725$ for $\Lambda=0.3$. We remind the reader that the value used in the Bonn model for this coupling is $\Lambda_{Bonn}=1.3$.

Quite surprisingly, in the strong binding limit ($B=0.5$) we have found $\alpha_{LFD}=1462$ and $\alpha_{NR}=3065$. Relativistic effects

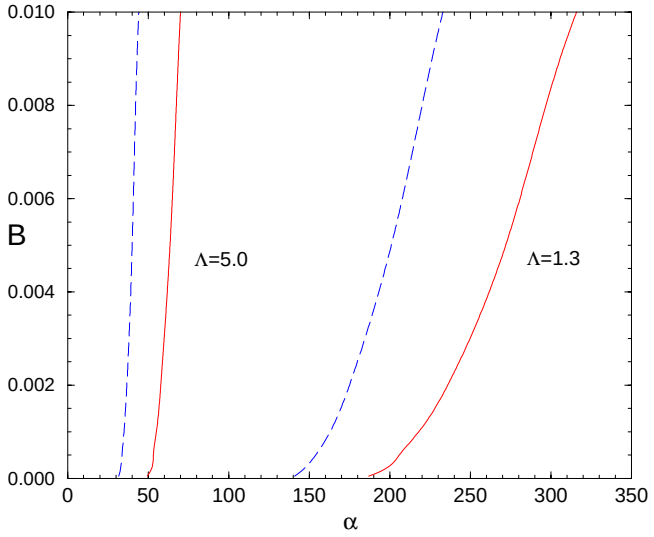

FIG. 13. $B(\alpha)$ for pseudoscalar coupling and $J^{\pi}=0^{+}$ state with $\mu=0.5$ and two different form factors compared to nonrelativistic results.

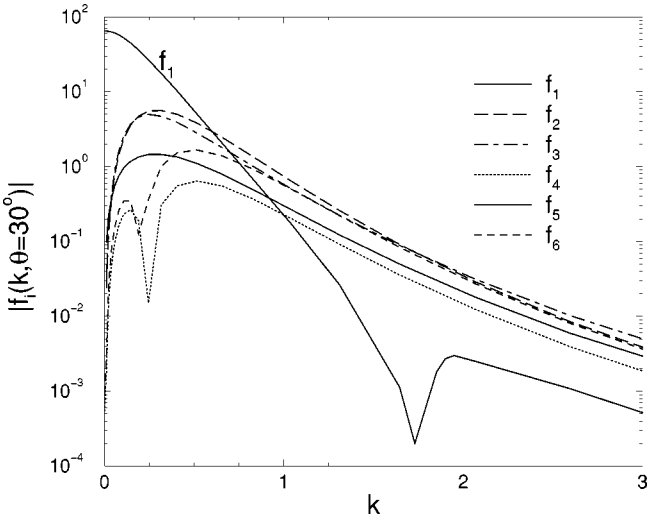

FIG. 14. Physical solutions for $J=1^{+}$ state with PS coupling. Parameters are $\alpha=60$, $\mu=0.25$, and $\Lambda=1.3$. Corresponding binding energy is $B=0.079$ and components are plotted for $\theta=30°$.

now become strongly attractive ($\alpha_{LFD}<\alpha_{NR}$). An essential part of this attraction is due to the coupling of the two f_1-f_2 components in the LFD wave function. By performing one-channel calculations, one has indeed $\alpha_{LFD}=3001$, which represents a strong reduction in the effect though it remains slightly attractive. We have checked if this attractive effect happens for different values of the exchange mass μ. For the same binding energy ($B=0.5$) and $\mu=0.5$ we have found $\alpha_{LFD}=1728$ and $\alpha_{NR}=1400$, repulsive once again. It is worth noting that for this coupling α_{NR} is a decreasing function of μ whereas α_{LFD} increases, at least in this energy region. This indicates to us the difficulty in discussing the "sign of relativistic effects" in general. They turn to depend not only on the kind of coupling but also on the binding energy of the system and, furthermore, on the mass of the exchanged particle.

It is interesting to study the zero binding limit of the LFD results and to compare them with the nonrelativistic ones. The NR potential (82) has been modified by including the Bonn form factor (18). The results are given in Fig. 13 for an exchange mass $\mu=0.5$ and with two different cutoff parameters Λ in the form factors. They show the same behavior that was found in the scalar case [64], i.e., the relativistic and nonrelativistic approaches do not coincide even when describing systems with zero binding energies as long as they interact with massive exchanges.

The $J=1$ state displays the same kind of departures from the scalar case as $J=0$. Functions $g_i^{(a)}$ for $a=0,1$ have been calculated using the values $\alpha_{PS}=60$, $\mu=0.25$, and $\Lambda=1.3$. Contrary to the scalar case, binding energies are sizably different: $B_{a=0}=0.103$ whereas $B_{a=1}=0.0494$. The physical wave function is obtained using the same procedure as for the scalar case, i.e., compute $f_{i=1,6}^{a=0,1}$ and extract from them the coefficients c_i. Their values, $c_0=0.749$ and $c_1=0.662$, are different from $c_0\approx 1/\sqrt{3}$ and $c_1\approx\sqrt{2/3}$, with c_0 larger than c_1. The averaged binding energy is $B=0.0793$. The corresponding solutions are plotted in Fig. 14. One can see that f_1 dominates at small momenta ($k\ll 1$), but starting from $k\sim 1$ the components of relativistic origin become larger than f_1.

The splitting in binding energies is much larger than for the scalar coupling. It can be seen in Fig. 15(a) where the results of $B_a(\alpha)$ for both $\hat{A}^2$ eigenstates are plotted. The energy differences remain important even in the $B\to 0$ limit, Fig. 15(b), in accordance with the analytical considerations in Sec. VI.

In summary, as was noted in Sec. VI, pseudoscalar coupling displays the largest deviations with respect to the nonrelativistic dynamics. Small and large spinor components are mixed to the first order. The coupling between f_1 and f_2 is essential even for very weakly bound systems, the components of relativistic origin dominate already at moderate values of k, and the splittings of the binding energies for the different projections of the $J\neq 0$ states are of the same order as the energies themselves.

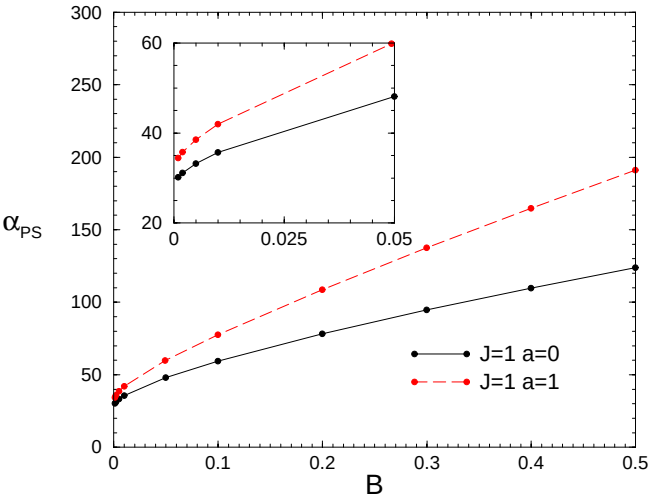

FIG. 15. Splitting of the $J=1$ solutions for pseudoscalar coupling. Results correspond to $\mu=0.25$ and $\Lambda=1.3$, $n=1$.

TABLE I. Coupling constant α as a function of the sharp cutoff k_{max} for the $J=0^-$ positronium state with binding energy $B=0.0225$ a.u.

k_{max}	10	20	30	40	50	70	100	200	300
α	0.3945	0.3928	0.3918	0.3911	0.3905	0.3896	0.3887	0.3867	0.3854

IX. RESULTS FOR VECTOR COUPLING

The stability analysis applied to vector kernels shows that vertex form factors are required for both $J=0^+$ and $J=1^+$ states to obtain stable solutions.

This is true in particular in the simplest application of vector coupling: the positronium $J=0^-$ state. The negative parity of the state comes from the intrinsic positron parity so that the corresponding kernels are those of the $J^\pi=0^+$ two-fermion system already given in Appendix A. In Table I the values of the coupling constant α are presented as a function of the sharp cutoff k_{max} and for a fixed binding energy $B=0.0225$. The dependence is very slow—0.3% variation for $k_{max}\in[10,300]$—but it actually corresponds to a logarithmic divergence of $\alpha(k_{max})$ as it can be seen in Fig. 16. The origin of this instability is the coupling to the second component, whose kernel matrix element κ_{22} has an attractive, constant asymptotic limit. If one removes this component—which has a very small contribution in norm—calculations become stable and give for $\alpha_{NR}=0.30$ the value $\alpha_{LFD}=0.3975$.

The comparison of LFD ladder results with those obtained in perturbative QED or to the physical energies is meaningless due to the instability of the solutions themselves. The use of vertex form factors in a system of pointlike particles would be hazardous and the introduction of renormalizable counterterms seems to be a more appropriate cure.

First positronium results in light-front dynamics were obtained in Refs. [37,38]. These authors introduced a large number of states in the Fock expansion but observed the same instability of the solutions. For a fixed value of the cutoff, the results become finite and can be compared. By taking $k_{max}=10$ and $\alpha=0.3$—which corresponds to $B_{NR}=0.0225$—we found $B_{LFD}=0.0132$, i.e., repulsive relativistic effects. The leading order QED corrections [79] read

$$B_{QED}=\frac{\alpha^2}{4}\left[1+\frac{21}{16}\alpha^2+o(\alpha^4)\right]\approx 0.02516,$$

and are attractive. Equation (10) from Ref. [38] gives for $k_{max}=10$ the value $B_{DLC}=0.0308$, in qualitative agreement—thought still sizably different—with B_{QED}. We should notice that a recent work [39] analyzes the results of Ref. [38] in terms of flow equations and obtains a closer value $B_{DLC}=0.02341$. We conclude from this that the ladder LFD predictions for such a genuine system are unable to reproduce even the sign of first order relativistic corrections. Because the lowest-order corrections of the singlet state are not affected by the annihilation channels, the differences could be due to cross ladder graphs.

For $\mu\neq 0$, the two-fermion system is bound due to the μ-dependent terms $[\sim(tt'/\mu^2)v_{ij}]$ in the vector kernel (A8), since the μ-independent ones (χ_{ij}) are repulsive. This binding disappears in the nonrelativistic limit.

When solving the equations for $J=0^+$ state, the standard form factors (18)—depending on Q^2 and local in the nonrelativistic limit—were found to be insufficient for any power n to ensure a stable solution. A Q^2 dependent Gaussian form factor failed as well. This unstability comes from the μ-dependent terms. These are off-shell corrections depending on variables t,t' defined by

$$4m^2t=4\varepsilon_k^2-M^2,\quad 4m^2t'=4\varepsilon_{k'}^2-M^2, \tag{98}$$

and are not regularized by a form factor depending on variable Q^2. Such a function cuts off the high $|\vec{k}-\vec{k}'|$ components, but not the $|\vec{k}+\vec{k}'|$ ones. A similar situation is encountered in the framework of chiral perturbation theory [80] and was solved by the replacement $\kappa(k,k')\rightarrow F(k)\kappa(k,k')F(k')$.

Our way of doing it is as follows. Variable $Q^2=-(k_{meson}-\omega\tau_1)^2$ entering $F(Q^2)$ is associated with the off-energy shell effects in the intermediate state containing one massive meson μ. In a similar way, we introduce the variable $\eta=m^2-(k_1-\omega\tau)^2$— see vertex 2 in the first graph of Fig. 3—and correspondingly $\eta'=m^2-(k'_2-\omega\tau')^2$ from vertex 1. Variables η and η' control the off-energy-shell contribution to the fermion states and have been regularized by means of a cutoff function

$$H(\eta)=\left(\frac{\Lambda^2}{\Lambda^2+\eta}\right)^n.$$

This corresponds to a nonlocal form factor even in the nonrelativistic limit. On energy shell one has $\eta=\eta'=0$.

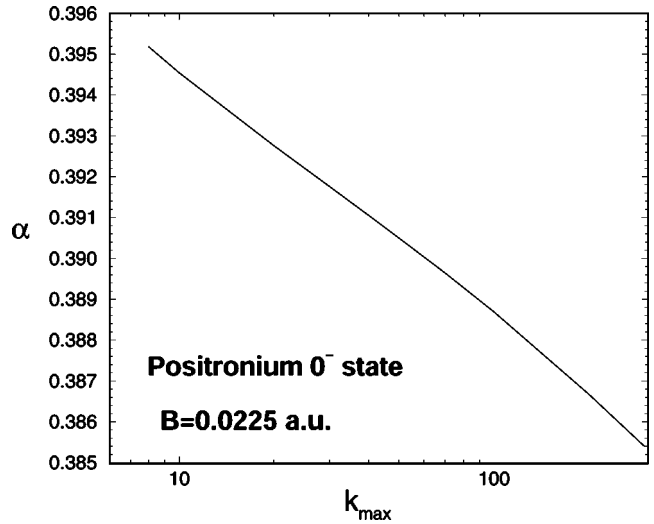

FIG. 16. Coupling constant α as a function of the sharp cutoff k_{max} for the $J=0^-$ positronium state with binding energy $B=0.0225$ a.u.

Thus, for instance, the total form factor associated with vertex 2 of Fig. 3 reads

$$F_{nloc}(Q^2,\,\eta) = F(Q^2)H(\eta). \tag{99}$$

In center of mass variables (3) the expressions for η, η' are

$$\eta = \begin{cases} \left(1 - \dfrac{\vec{k}\cdot\vec{n}}{\varepsilon_k}\right) 2m^2 t \text{ if } \dfrac{\vec{k}'\cdot\vec{n}}{\varepsilon_{k'}} - \dfrac{\vec{k}\cdot\vec{n}}{\varepsilon_k} > 0 \\ \left(1 + \dfrac{\vec{k}\cdot\vec{n}}{\varepsilon_k}\right) 2m^2 t \text{ if } \dfrac{\vec{k}'\cdot\vec{n}}{\varepsilon_{k'}} - \dfrac{\vec{k}\cdot\vec{n}}{\varepsilon_k} < 0 \end{cases} \tag{100}$$

and

$$\eta' = \begin{cases} \left(1 + \dfrac{\vec{k}'\cdot\vec{n}}{\varepsilon_{k'}}\right) 2m^2 t' \text{ if } \dfrac{\vec{k}'\cdot\vec{n}}{\varepsilon_{k'}} - \dfrac{\vec{k}\cdot\vec{n}}{\varepsilon_k} > 0 \\ \left(1 - \dfrac{\vec{k}'\cdot\vec{n}}{\varepsilon_{k'}}\right) 2m^2 t' \text{ if } \dfrac{\vec{k}'\cdot\vec{n}}{\varepsilon_{k'}} - \dfrac{\vec{k}\cdot\vec{n}}{\varepsilon_k} < 0, \end{cases} \tag{101}$$

with t, t' given defined in Eq. (98).

Each coupling constant is replaced by $g \to gF(Q^2)H(\eta)$—or $g \to gF(Q^2)H(\eta')$—and the kernel is multiplied by $F^2(Q^2)H(\eta)H(\eta')$. The values for Λ and n in H are taken the same as for $F(Q^2)$, but could in principle be different.

By means of Eq. (99), the solutions become stable but we notice that the use of only one kind of form factor is not enough to ensure the stability. Wave functions corresponding to μ=0.15 obtained with n=1 and Λ=1.3 in Eq. (99) are displayed in Fig. 17. Binding energy is B=0.0225 and α_v =1.485. They have normal behavior and one notices sizable relativistic component f_2 starting from $k \approx 0.5$ with a strong θ dependence despite the small binding energy of the state.

Let us now consider the $J^\pi = 1^+$ state. Solving the $J^\pi = 1^+, a = 0$ equations with the $F(Q^2)$ form factor only leads to the same anomalies as for $J^\pi = 0^+$. With the nonlocal form factor the situation is regularized. With parameters B =0.050, μ=0.25, Λ=1.3, and n=1, for instance, one has a coupling constant α=6.18 and a well behaved wave function. The same happens for the $J^\pi = 1^+, a = 1$ state. When using, with the same parameters, the nonlocal form factor (99), we get α=6.01.

The mass splitting between the two $a = 0, 1$ projections is shown in Fig. 18. One first notices the striking behavior of $\alpha_a(B)$ curves, i.e., larger binding energies correspond to smaller values of the coupling constant α. This fact—which takes place also for $J=0^+$ states—is a consequence of the M^2 dependence of the tt'/μ^2 terms driving the vector kernel $\kappa_{ij}^{(\mu)}$ in Eq. (A8). Its contribution is large because of μ^2 in the denominator. Increasing the binding energy—i.e., decreasing M^2—increases t, t' factors and results in smaller values of α. When the M^2 dependence in t, t' kernel is frozen—setting, e.g., $M^2 = 4m^2$ —the usual $\alpha(B)$ variation is recovered (dotted curve in Fig. 18). When including the full dynamics, both $\alpha_a(B)$ curves get close to each other in all the variation domain B=[0, 0.5], as was the case in the scalar coupling. However due to their peculiar behavior—flat and almost parallel—the splitting in binding energies corresponding to a fixed value of the coupling constant can be very large. One can also notice in Fig. 18 the different values of α_a at B=0, despite the fact that the systems of equations for a=0 and a=1 have—as in the scalar coupling—the same nonrelativistic limit. This difference is due to the $1/\mu^2$ terms in the kernel. They are not relevant at the $(1/m)^0$ order but are crucial for binding a relativistic two-fermion system by vector exchange. For a fermion-antifermion system with massless exchange, e.g., positronium, the splitting at B=0 disappears.

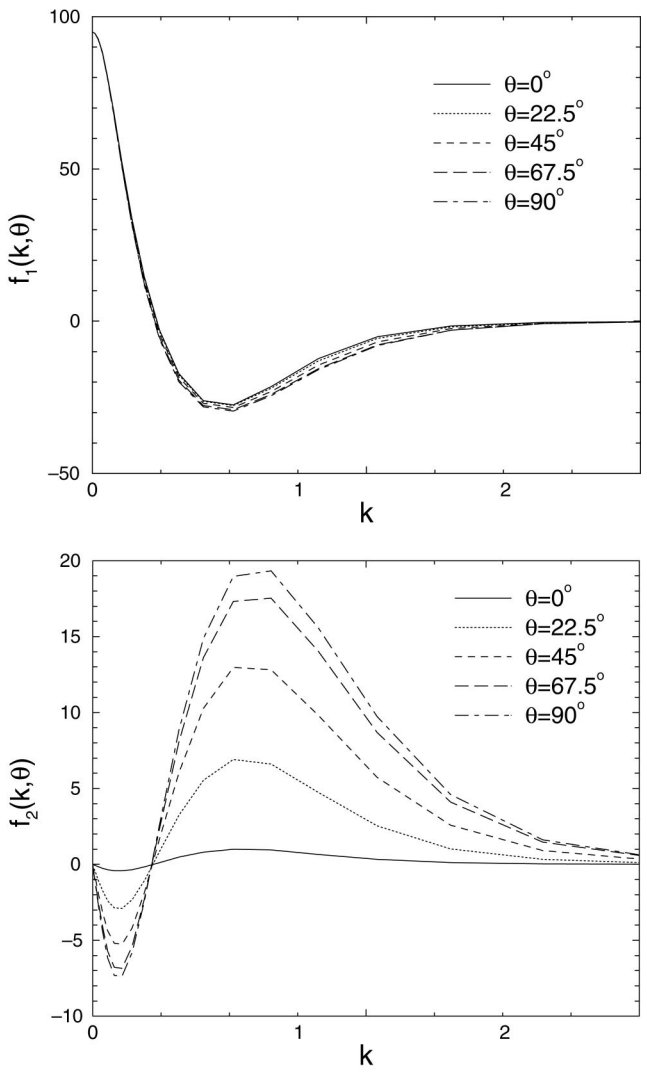

FIG. 17. Wave functions f_i for a $J^\pi = 0^+$ state in the vector coupling with μ=0.15 and using the nonlocal form factor (99) with n =1 and Λ=1.3. The coupling constant is α=1.485 and the binding energy B=0.0225.

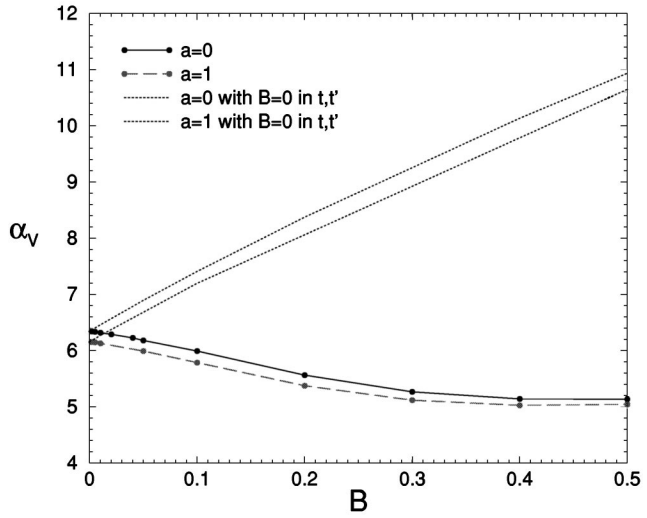

FIG. 18. Splitting of the $J=1^+$ solutions for vector coupling with $\mu=0.25$ and form factors (99) with $\Lambda=1.3$ $n=1$. Dotted lines correspond to a fixed binding energy ($B=0$) in t,t' off-shell variables of kernel (A8).

X. CONCLUSION

We have presented the explicitly covariant LFD solutions for the bound state of two-fermion systems in the ladder approximation. A method for constructing nonzero angular momentum states has been proposed and illustrated by numerical examples. It is based on satisfying the angular condition by a linear superposition of eigenstates of an operator commuting with the LFD ladder Hamiltonian.

We have separately examined the different types of OBE couplings and found very different behaviors concerning the stability of the solutions themselves and their relation with the corresponding nonrelativistic reductions.

Scalar coupling (Yukawa model) is found to be stable without any kernel regularization for the $J^\pi=0^+$ state and coupling constants below some critical value $\alpha<\alpha_c=3.72$. For values above α_c the system collapses. For the $J^\pi=1^+$ state the solutions of both $a=0$ and $a=1$ projections are unstable. Their energy splitting is very small even for binding energies B of the same order as the constituent mass and vanishes at $B=0$. The physical solution, satisfying the angular condition, has been constructed by a suitable linear combination of $a=0,1$ states. LFD binding energies are found to be close to those given by their nonrelativistic limit, even closer than the case of purely scalar particles (Wick Cutkosky model extended to $\mu\neq 0$). The comparison with the nonrelativistic solutions always shows repulsive effects. The LFD wave function is dominated by the component which has a nonrelativistic counterpart. Extra components of relativistic origin remain negligible even at large values of the relative momentum ($k>m$).

Pseudoscalar coupling is also found stable for $J^\pi=0^+$ state. It displays a very strong dependence of binding energies as a function of the coupling constant: they vary from $B=0.001$ to $B=0.500$ (in constituent mass units) while the coupling constant changes from $\alpha=55.5$ to $\alpha=58.5$. This dependence is due to the coupling to the wave function component of relativistic origin. Vertex form factors are required for $J^\pi=1^+$ states. LFD solutions, obtained with regularized kernels, present large deviations with respect to nonrelativistic case, even for weakly bound states, and display a big sensitivity to the cutoff parameters. The LFD wave function is dominated by a relativistic component at relatively small momenta ($k<m$). The coupling between different components is strongly attractive and can compensate the repulsive effects observed in the Yukawa model. Thus, relativistic corrections can be attractive or repulsive depending on the quantum number of state, the value of the binding energy, and even the mass μ of the exchanged meson. The energy splitting between different projections of $J=1$ states is large and remains at $B=0$.

Vector coupling presents stronger anomalies. For $\mu=0$ it has been applied to the positronium 0^+ state. It is found to be unstable and, once regularized by means of sharp cutoff-off, the ladder approximation gives relativistic corrections of opposite sign compared to QED perturbative results. This failure shows the poorness of the ladder approximation in one of the rare cases in which it can be confronted with experimental results. For $\mu\neq 0$ the LFD solutions collapse even using local cutoff form factors. The reason lies in the strong nonlocalities of the μ-dependent terms in the LFD kernel. These terms have their origin in the massive vector propagator and manifest as off-shell corrections of the $\mu=0$ kernels. They have been regularized using appropriate vertex form factors. The $J=1^+$ state has thus been calculated. This state is not bound in the nonrelativistic limit and its existence in a relativistic approach is entirely due to the μ-dependent terms in the kernel. The importance of this off-shell terms is thus dramatic. In particular, their energy dependence generates a decrease of the binding energy as a function of the coupling constant, which questions the very meaning of the interaction strength. The $\alpha_a(B)$ dependence for different projections of $J=1$ states remain very close to each other even for $B\sim m$ but their particular form—smooth and almost parallel variation—can give rise to large energy splitting for a fixed value of the coupling constant.

Some general additional remarks concerning the relativistic calculations are given as follows.

(i) Contrary to the nonrelativistic case, vertex form factors are unavoidable in any realistic calculation. The full spinor structure generates highly singular kernels which are not regularized by local vertex form factors. It is clear that, especially at large k values, the obtained wave function and consequently the electromagnetic form factors will crucially depend on the way the regularization is performed. The large momentum components will thus be determined not by the dynamics but by uncontrolled parameters. We believe that here lies the main drawback of relativistic approaches.

(ii) The consequences of implementing the Lorentz invariance in a quantum mechanical description of a system are not only kinematical but mainly dynamical. Large differences with respect to the nonrelativistic solutions appear even in the zero binding limit for systems with $k/m\ll 1$ as long as the exchanged mass is nonzero. We have explicitly

shown for scalar and pseudoscalar couplings that the behavior of $\alpha(B)$ at $B\approx 0$ differs from their nonrelativistic counterparts, a result already found in the Wick-Cutkosky model [64].

(iii) The question about the sign of relativistic effects has no simple answer. They can be different, following the nature of the constituents, the kind of interaction, the quantum numbers of the state, its binding energy, and even the mass of the exchanged particle. This shows that there are no simple recipes to perform *a priori* evaluations.

(iv) The splitting of different projections of $J=1$ states is very different following the kind of coupling. In nuclear physics—where the weight of scalar mesons in the binding energy is dominating—it is expected to be very small. The same is true for the massless vector coupling such as one-photon or one-gluon exchange. It can be however very large in relativistic models where pseudoscalar exchange plays an important role.

Finally, we would like to emphasize one of the interesting features of using LFD in describing the relativistic composite systems. It lies in the fact that wave function components appearing in this approach are closely related to their nonrelativistic counterparts. Some of these components are the formal equivalent of the usual nonrelativistic solutions while the others are of pure relativistic origin. Relativity manifests both in modifying the former and in giving a sizable weight to the latter ones. We have found that the coupling between these components plays an essential role, even in determining the stability of the solutions. In addition—except for the scalar exchange—the total wave function is dominated by the relativistic components at moderate values of its arguments ($k<m$), even for loosely bound systems.

ACKNOWLEDGMENTS

One of the authors (V.A.K.) is sincerely grateful for the warm hospitality of the theory group at the Institut des Sciences Nucléaires de Grenoble, where this work was performed. Numerical calculations were carried out at CGCV (CEA Grenoble) and IDRIS (CNRS). We thank the staff members of these organizations for their constant support. This work was partially supported by the French-Russian PICS and RFBR Grant Nos. 1172 and 01-02-22002 as well as by the RFBR Grant No. 02-02-16809.

APPENDIX A: KERNELS

Kernels κ_{ij} are obtained from Eqs. (45), (46), (63), and (64) as traces of 4×4 matrices. To calculate these traces, it is useful to express the scalar products between all the concerned four-vectors in terms of variables (k, k', θ, θ'). They read

$$\omega^2 = 0,$$

$$k_1^2 = k_2^2 = k_1'^2 = k_2'^2 = m^2,$$

$$\omega\cdot k_1 = x\omega\cdot p,$$

$$\omega\cdot k_2 = (1-x)\omega\cdot p,$$

$$\omega\cdot k_1' = x'\omega\cdot p,$$

$$\omega\cdot k_2' = (1-x')\omega\cdot p,$$

$$k_1\cdot k_2 = 2\varepsilon_k^2 - m^2,$$

$$k_1'\cdot k_2' = 2\varepsilon_{k'}^2 - m^2,$$

$$k_1\cdot p = 2\varepsilon_k^2(1-x) + \tfrac{1}{2}M^2 x,$$

$$k_2\cdot p = 2\varepsilon_k^2 x + \tfrac{1}{2}M^2(1-x),$$

$$k_1'\cdot p = 2\varepsilon_{k'}^2(1-x') + \tfrac{1}{2}M^2 x',$$

$$k_2'\cdot p = 2\varepsilon_{k'}^2 x + \tfrac{1}{2}M^2(1-x'),$$

$$k_1\cdot k_1' = -kk'\ \sin\theta\sin\theta'\ \cos\phi + 2\varepsilon_{k'}^2 x + 2\varepsilon_k^2 x' - 2\varepsilon_k^2 xx' - 2\varepsilon_{k'}^2 xx',$$

$$k_2\cdot k_2' = -kk'\ \sin\theta\sin\theta'\ \cos\phi + 2\varepsilon_k^2 x + 2\varepsilon_{k'}^2 x' - 2\varepsilon_k^2 xx' - 2\varepsilon_{k'}^2 xx',$$

$$k_1\cdot k_2' = kk'\ \sin\theta\sin\theta'\ \cos\phi + 2\varepsilon_k^2(1-x)(1-x') + 2\varepsilon_{k'}^2 xx',$$

$$k_2\cdot k_1' = kk'\ \sin\theta\sin\theta'\ \cos\phi + 2\varepsilon_{k'}^2(1-x)(1-x') + 2\varepsilon_k^2 xx', \tag{A1}$$

where

$$x = \frac{1}{2}\left(1 - \frac{k}{\varepsilon_k}\cos\theta\right),\quad x' = \frac{1}{2}\left(1 - \frac{k'}{\varepsilon_{k'}}\cos\theta'\right). \tag{A2}$$

Using the above result, we have obtained the analytical expressions of κ_{ij} kernels for $J^\pi = 0^+, 1^+$ states. They are written below, coupling by coupling, in the form

$$\kappa_{ij}(k,\theta,k',\theta',\varphi') = c_{ij}(k,\theta,k',\theta') + d_{ij}(k,\theta,k',\theta')\cos\varphi' + e_{ij}(k,\theta,k',\theta')\cos^2\varphi', \tag{A3}$$

with coefficients c_{ij}, d_{ij}, e_{ij} invariant under the transformation $(i,k,\theta)\leftrightarrow(i',k',\theta')$. We introduce for shortness the notations

$$s\theta = \sin\theta,\quad c\theta = \cos\theta,\quad S\theta = k\sin\theta,\quad C\theta = k\cos\theta,$$
$$c\varphi' = \cos\varphi',$$

plus corresponding primed and the following quantities:

$$b_{\pm}^2 = m^2(\varepsilon_k^2 + \varepsilon_{k'}^2) \pm 2\varepsilon_k^2\varepsilon_{k'}^2,$$

$$\varepsilon_k^{\pm} = \varepsilon_k \pm m,$$

$$\Delta^{\pm} = \varepsilon_k^2 \pm \varepsilon_{k'}^2.$$

Coupling constants appear through $\alpha = g^2/4\pi$.

1. Scalar

Kernels for the scalar coupling were already given in Ref. [68] and are included here for completeness.

For $J=0^+$,

$$\frac{\kappa_{11}}{\alpha\pi} = -[m^2\Delta^+ + 2\varepsilon_k\varepsilon_{k'}(\varepsilon_k\varepsilon_{k'} - C\theta C\theta')] + \Delta^+ S\theta S\theta' c\varphi',$$

$$\frac{\kappa_{12}}{\alpha\pi} = -m\Delta^-(S\theta' + S\theta c\varphi'),$$

$$\frac{\kappa_{21}}{\alpha\pi} = +m\Delta^-(S\theta + S\theta' c\varphi'), \tag{A4}$$

$$\frac{\kappa_{22}}{\alpha\pi} = \Delta^+ S\theta S\theta' - [m^2\Delta^+ + 2\varepsilon_k\varepsilon_{k'}(\varepsilon_k\varepsilon_{k'} - C\theta C\theta')]c\varphi'.$$

For $J=1^+$, $a=0$,

$$\frac{\kappa_{11}}{\alpha\pi} = [2kk'\varepsilon_k\varepsilon_{k'} - b_+^2 c\theta c\theta'] - \varepsilon_k\varepsilon_{k'}\Delta^+ s\theta s\theta' c\varphi', \tag{A5}$$

$$\frac{\kappa_{12}}{\alpha\pi} = m\varepsilon_{k'}(2\varepsilon_k^2 + \Delta^+)c\theta s\theta' - m\varepsilon_k(2\varepsilon_{k'}^2 + \Delta^+)s\theta c\theta' c\varphi',$$

$$\frac{\kappa_{21}}{\alpha\pi} = m\varepsilon_k(2\varepsilon_{k'}^2 + \Delta^+)s\theta c\theta' - m\varepsilon_{k'}(2\varepsilon_k^2 + \Delta^+)c\theta s\theta' c\varphi',$$

$$\frac{\kappa_{22}}{\alpha\pi} = -\varepsilon_k\varepsilon_{k'}\Delta^+ s\theta s\theta' + [2kk'\varepsilon_k\varepsilon_{k'} - b_+^2 c\theta c\theta']c\varphi'.$$

For $J=1^+$, $a=1$,

$$\frac{2\kappa_{11}}{\alpha\pi} = -\{m\varepsilon_k s^2\theta(\Delta^+ + 2\varepsilon_{k'}^2) + m\varepsilon_{k'}s^2\theta'(\Delta^+ + 2\varepsilon_k^2) + (c^2\theta + c^2\theta')b_+^2 - 4\varepsilon_k\varepsilon_{k'}C\theta C\theta'\} - \{\Delta^+(\varepsilon_k^-\varepsilon_{k'}^- c\theta c\theta' - kk')s\theta s\theta'\}c\varphi' - \{\Delta^+\varepsilon_k^-\varepsilon_{k'}^- s^2\theta s^2\theta'\}c^2\varphi',$$

$$\frac{2\kappa_{12}}{\alpha\pi} = [m\varepsilon_k(\Delta^+ + 2\varepsilon_{k'}^2) - b_+^2]s^2\theta - [m\varepsilon_{k'}(\Delta^+ + 2\varepsilon_k^2) - b_+^2]s^2\theta' - \{kk'(\varepsilon_k - \varepsilon_{k'})^2 + (\varepsilon_k + \varepsilon_{k'})^2\varepsilon_k^-\varepsilon_{k'}^- c\theta c\theta'\}s\theta s\theta' c\varphi' + \{\varepsilon_{k'}^-(\varepsilon_k + \varepsilon_{k'})^2 c^2\theta' - \varepsilon_{k'}^+(\varepsilon_k - \varepsilon_{k'})^2\}\varepsilon_k^- s^2\theta c^2\varphi',$$

$$\frac{\sqrt{2}\kappa_{13}}{\alpha\pi} = -2\varepsilon_k\varepsilon_{k'}C\theta S\theta' - \varepsilon_{k'}^-(m\Delta^+ - 2\varepsilon_k^2\varepsilon_{k'})c\theta' s\theta' + \{2\varepsilon_k\varepsilon_{k'}kC\theta' + \varepsilon_k^- c\theta[\varepsilon_{k'}(\Delta^+ - 2m\varepsilon_k) - \varepsilon_{k'}^-(\varepsilon_k + \varepsilon_{k'})^2 c^2\theta']\}s\theta c\varphi' - (\varepsilon_k + \varepsilon_{k'})^2\varepsilon_k^-\varepsilon_{k'}^- s^2\theta s\theta' c\theta' c^2\varphi',$$

$$\frac{\sqrt{2}\kappa_{14}}{\alpha\pi} = \Delta^-\{(m + \varepsilon_k^- s^2\theta)S\theta' + mS\theta c\varphi' - \varepsilon_k^- s^2\theta S\theta' c^2\varphi'\},$$

$$\frac{2\kappa_{21}}{\alpha\pi} = [m\varepsilon_{k'}(\Delta^+ + 2\varepsilon_k^2) - b_+^2]s^2\theta' - [m\varepsilon_k(\Delta^+ + 2\varepsilon_{k'}^2) - b_+^2]s^2\theta - \{kk'(\varepsilon_k - \varepsilon_{k'})^2 + (\varepsilon_k + \varepsilon_{k'})^2\varepsilon_{k'}^-\varepsilon_k^- c\theta c\theta'\}s\theta s\theta' c\varphi' + \{\varepsilon_k^-(\varepsilon_{k'} + \varepsilon_k)^2 c^2\theta - \varepsilon_k^+(\varepsilon_{k'} - \varepsilon_k)^2\}\varepsilon_{k'}^- s^2\theta' c^2\varphi',$$

$$\frac{2\kappa_{22}}{\alpha\pi} = m(\varepsilon_k + \varepsilon_{k'})^3 - \varepsilon_k^-(m\Delta^+ - 2\varepsilon_k\varepsilon_{k'}^2)c^2\theta - \varepsilon_{k'}^-(m\Delta^+ - 2\varepsilon_k^2\varepsilon_{k'})c^2\theta' - 4\varepsilon_k\varepsilon_{k'}C\theta C\theta' - (\varepsilon_k + \varepsilon_{k'})^2(\varepsilon_k^-\varepsilon_{k'}^- - C\theta C\theta')s\theta s\theta' c\varphi' - \{2b_+^2(c^2\theta + c^2\theta') + 2m[\varepsilon_k(\Delta^+ + 2\varepsilon_{k'}^2)s^2\theta + \varepsilon_{k'}(\Delta^+ + 2\varepsilon_k^2)s^2\theta'] + (\varepsilon_k + \varepsilon_{k'})^2\varepsilon_k^-\varepsilon_{k'}^- s^2\theta s^2\theta' - 8\varepsilon_k\varepsilon_{k'}C\theta C\theta'\}c^2\varphi',$$

$$\frac{\sqrt{2}\kappa_{23}}{\alpha\pi} = \{2k'\varepsilon_k\varepsilon_{k'}C\theta + \varepsilon_{k'}^-(m\Delta^+ - 2\varepsilon_k^2\varepsilon_{k'})c\theta'\}s\theta' - \{\varepsilon_k^- c\theta[\varepsilon_{k'}^-(\varepsilon_k + \varepsilon_{k'})^2 c^2\theta' - \varepsilon_{k'}(\Delta^+ - 2m\varepsilon_k)] - 2k\varepsilon_k\varepsilon_{k'}C\theta'\}s\theta c\varphi' - \{\varepsilon_{k'}^- c\theta'((\varepsilon_k - \varepsilon_{k'})^2\varepsilon_k^+ - (\varepsilon_k + \varepsilon_{k'})^2\varepsilon_k^- c^2\theta) + 4k'\varepsilon_k\varepsilon_{k'}C\theta\}s\theta' c^2\varphi',$$

$$\frac{\sqrt{2}\kappa_{24}}{\alpha\pi} = +\Delta^-\{(\varepsilon_k - \varepsilon_k^- c^2\theta)S\theta' - mS\theta c\varphi' - (\varepsilon_k^+ - \varepsilon_k^- c^2\theta)S\theta' c^2\varphi'\},$$

$$\frac{\sqrt{2}\kappa_{31}}{\alpha\pi} = -2\varepsilon_k\varepsilon_{k'}S\theta C\theta' - \varepsilon_k^-(m\Delta^+ - 2\varepsilon_k\varepsilon_{k'}^2)s\theta c\theta + s\theta'\{\varepsilon_k^- c\theta'[(m\Delta^+ - 2\varepsilon_k^2\varepsilon_{k'})c^2\theta + \varepsilon_k(\Delta^+ - 2m\varepsilon_{k'})s^2\theta] + 2\varepsilon_k\varepsilon_{k'}kC\theta'\}c\varphi' - \Delta^+\varepsilon_k^-\varepsilon_{k'}^- s\theta c\theta s^2\theta' c^2\varphi',$$

$$\frac{\sqrt{2}\kappa_{32}}{\alpha\pi} = \{2k\varepsilon_k\varepsilon_{k'}C\theta' + \varepsilon_k^-(m\Delta^+ - 2\varepsilon_k\varepsilon_{k'}^2)c\theta\}s\theta - \{\varepsilon_{k'}^- c\theta'[\varepsilon_k^-(\varepsilon_k+\varepsilon_{k'})^2c^2\theta - \varepsilon_k(\Delta^+ - 2m\varepsilon_{k'})] - 2k'\varepsilon_k\varepsilon_{k'}C\theta\}s\theta' c\varphi' - \{\varepsilon_k^- c\theta[(\varepsilon_k-\varepsilon_{k'})^2\varepsilon_{k'}^+ - (\varepsilon_k+\varepsilon_{k'})^2\varepsilon_{k'}^- c^2\theta'] + 4k\varepsilon_k\varepsilon_{k'}C\theta'\}s\theta c^2\varphi',$$

$$\frac{\kappa_{33}}{\alpha\pi} = \{\varepsilon_k\varepsilon_{k'}^-(\Delta^+ - 2m\varepsilon_{k'})c^2\theta' + \varepsilon_{k'}\varepsilon_k^-(\Delta^+ - 2m\varepsilon_k)c^2\theta - \varepsilon_k\varepsilon_{k'}(\Delta^+ + 2m^2) - [(\varepsilon_k+\varepsilon_{k'})^2\varepsilon_k^-\varepsilon_{k'}^- c\theta c\theta' - 2kk'\varepsilon_k\varepsilon_{k'}]c\theta c\theta'\}c\varphi' - [(\varepsilon_k+\varepsilon_{k'})^2\varepsilon_k^-\varepsilon_{k'}^- c\theta c\theta' - 2kk'\varepsilon_k\varepsilon_{k'}]s\theta s\theta' c^2\varphi',$$

$$\frac{\kappa_{34}}{\alpha\pi} = +\Delta^-\varepsilon_k^- s\theta c\theta S\theta'(1-c^2\varphi'),$$

$$\frac{\sqrt{2}\kappa_{41}}{\alpha\pi} = -\Delta^-\{(m+\varepsilon_{k'}^- s^2\theta')S\theta + mS\theta' c\varphi' - \varepsilon_{k'}^- s^2\theta' S\theta c^2\varphi'\},$$

$$\frac{\sqrt{2}\kappa_{42}}{\alpha\pi} = -\Delta^-\{(\varepsilon_{k'} - \varepsilon_{k'}^- c^2\theta')S\theta - mS\theta' c\varphi' - (\varepsilon_{k'}^+ - \varepsilon_{k'}^- c^2\theta')S\theta c^2\varphi'\},$$

$$\frac{\sqrt{2}\kappa_{42}}{\alpha\pi} = -\Delta^-\{(\varepsilon_{k'} - \varepsilon_{k'}^- c^2\theta')S\theta - mS\theta' c\varphi' - (\varepsilon_{k'}^+ - \varepsilon_{k'}^- c^2\theta')S\theta c^2\varphi'\},$$

$$\frac{\kappa_{43}}{\alpha\pi} = -\Delta^-\varepsilon_{k'}^- s\theta' c\theta' S\theta(1-c^2\varphi'),$$

$$\frac{\kappa_{44}}{\alpha\pi} = [2\varepsilon_k\varepsilon_{k'}(C\theta C\theta' - \varepsilon_k\varepsilon_{k'}) - m^2\Delta^+]c\varphi' + \Delta^+ S\theta S\theta' c^2\varphi'.$$

2. Pseudoscalar

For $J=0^+$,

$$\frac{\kappa_{11}}{\alpha\pi} = -[m^2\Delta^+ - 2\varepsilon_k\varepsilon_{k'}(\varepsilon_k\varepsilon_{k'} - C\theta C\theta')] + \Delta^+ S\theta S\theta' c\varphi',$$

$$\frac{\kappa_{12}}{\alpha\pi} = -m\Delta^-(S\theta' - S\theta c\varphi'),$$

$$\frac{\kappa_{21}}{\alpha\pi} = +m\Delta^-(S\theta - S\theta' c\varphi'), \tag{A6}$$

$$\frac{\kappa_{22}}{\alpha\pi} = \Delta^+ S\theta S\theta' + [m^2\Delta^+ - 2\varepsilon_k\varepsilon_{k'}(\varepsilon_k\varepsilon_{k'} - C\theta C\theta')]c\varphi'.$$

For $J=1$, $a=0$,

$$\frac{\kappa_{11}}{\alpha\pi} = -(2kk'\varepsilon_k\varepsilon_{k'} + b_-^2 c\theta c\theta') + \varepsilon_k\varepsilon_{k'}(\Delta^+ - 2m^2)s\theta s\theta' c\varphi',$$

$$\frac{\kappa_{12}}{\alpha\pi} = -m\Delta^-(\varepsilon_{k'}c\theta s\theta' - \varepsilon_k s\theta c\theta' c\varphi'),$$

$$\frac{\kappa_{21}}{\alpha\pi} = +m\Delta^-(\varepsilon_k s\theta c\theta' - \varepsilon_{k'}c\theta s\theta' c\varphi'), \tag{A7}$$

$$\frac{\kappa_{22}}{\alpha\pi} = -\varepsilon_k\varepsilon_{k'}(\Delta^+ - 2m^2)s\theta s\theta' + (2kk'\varepsilon_k\varepsilon_{k'} + b_-^2 c\theta c\theta')c\varphi'.$$

For $J=1^+$, $a=1$,

$$\frac{2\kappa_{11}}{\alpha\pi} = 4C\theta C\theta'\varepsilon_k\varepsilon_{k'} + m\Delta^-(\varepsilon_k s^2\theta - \varepsilon_{k'}s^2\theta') + b_-^2(c^2\theta + c^2\theta') + (\varepsilon_k-\varepsilon_{k'})^2(kk' - \varepsilon_k^-\varepsilon_{k'}^- c\theta c\theta')s\theta s\theta' c\varphi' + (\varepsilon_k - \varepsilon_{k'})^2\varepsilon_k^-\varepsilon_{k'}^- s^2\theta s^2\theta' c^2\varphi',$$

$$\frac{2\kappa_{12}}{\alpha\pi} = (c^2\theta - c^2\theta')b_-^2 - m\Delta^-(\varepsilon_k s^2\theta + \varepsilon_{k'}s^2\theta') - \{kk'(\varepsilon_k+\varepsilon_{k'})^2 + c\theta c\theta'(\varepsilon_k-\varepsilon_{k'})^2\varepsilon_k^-\varepsilon_{k'}^-\}s\theta s\theta' c\varphi' - \{(b_-^2 - m\varepsilon_k\Delta^-)(1+c^2\theta') + \varepsilon_{k'}\varepsilon_k^-(\Delta^+ + 2m\varepsilon_k)s^2\theta'\}s^2\theta c^2\varphi',$$

$$\frac{\sqrt{2}\kappa_{13}}{\alpha\pi} = \{[\varepsilon_{k'}(\Delta^- + 2m\varepsilon_k) - \varepsilon_{k'}^-(\varepsilon_k-\varepsilon_{k'})^2c^2\theta']\varepsilon_k^- c\theta - 2k\varepsilon_k\varepsilon_{k'}C\theta'\}s\theta c\varphi' - \{(b_-^2 + m\varepsilon_{k'}\Delta^-)c\theta' + 2kk'\varepsilon_k\varepsilon_{k'}c\theta\}s\theta' + \varepsilon_k^-\varepsilon_{k'}^-(\varepsilon_k-\varepsilon_{k'})^2s^2\theta s\theta' c\theta' c^2\varphi',$$

$$\frac{\sqrt{2}\kappa_{14}}{\alpha\pi} = \Delta^-\{-(\varepsilon_k - \varepsilon_k^+ c^2\theta)S\theta' + mS\theta c\varphi' + \varepsilon_k^- s^2\theta S\theta' c^2\varphi'\},$$

$$\frac{2\kappa_{21}}{\alpha\pi} = (c^2\theta - c^2\theta')b_-^2 + m\Delta^-(\varepsilon_k s^2\theta + \varepsilon_{k'}s^2\theta') - \{kk'(\varepsilon_k+\varepsilon_{k'})^2 + c\theta c\theta'(\varepsilon_k-\varepsilon_{k'})^2\varepsilon_k^-\varepsilon_{k'}^-\}s\theta s\theta' c\varphi' - \{(b_-^2 + m\varepsilon_{k'}\Delta^-)(1+c^2\theta) + \varepsilon_k\varepsilon_{k'}^-(\Delta^+ + 2m\varepsilon_{k'})s^2\theta\}s^2\theta' c^2\varphi',$$

$$\frac{2\kappa_{22}}{\alpha\pi} = -m\Delta^-(\varepsilon_k s^2\theta - \varepsilon_{k'} s^2\theta') - b_-^2(c^2\theta + c^2\theta') - 4\varepsilon_k\varepsilon_{k'} C\theta C\theta' + \{kk'(\varepsilon_k - \varepsilon_{k'})^2 + c\theta c\theta'[m\Delta^-(\varepsilon_k - \varepsilon_{k'}) - b_-^2 - \varepsilon_k\varepsilon_{k'}(\Delta^+ - 2m^2)]\} s\theta s\theta' c\varphi' + \{8\varepsilon_k\varepsilon_{k'} C\theta C\theta' + 2b_-^2(c^2\theta + c^2\theta') + 2m\Delta^-(\varepsilon_k s^2\theta - \varepsilon_{k'} s^2\theta') + s^2\theta s^2\theta'(\varepsilon_k - \varepsilon_{k'})^2\varepsilon_k^-\varepsilon_{k'}^-\} c^2\varphi',$$

$$\frac{\sqrt{2}\kappa_{23}}{\alpha\pi} = \{2k'\varepsilon_k\varepsilon_{k'} C\theta + (b_-^2 + m\varepsilon_{k'}\Delta^-)c\theta'\} s\theta' + \{[\varepsilon_{k'}(\Delta^+ + 2m\varepsilon_k)s^2\theta' + (m\Delta^+ + 2\varepsilon_k\varepsilon_{k'}^2)c^2\theta']\varepsilon_k^- c\theta - 2k\varepsilon_k\varepsilon_{k'} C\theta'\} s\theta c\varphi' + \{[\varepsilon_k(\Delta^+ + 2m\varepsilon_{k'})s^2\theta + (m\Delta^+ + 2\varepsilon_k^2\varepsilon_{k'})(1 + c^2\theta)]\varepsilon_{k'}^- c\theta' - 4k'\varepsilon_k\varepsilon_{k'} C\theta\} s\theta' c^2\varphi',$$

$$\frac{\sqrt{2}\kappa_{24}}{\alpha\pi} = -\Delta^-\{(\varepsilon_k - c^2\theta\varepsilon_k^-)S\theta' + mS\theta c\varphi' - (\varepsilon_k^+ - \varepsilon_k^- c^2\theta)S\theta' c^2\varphi'\},$$

$$\frac{\sqrt{2}\kappa_{31}}{\alpha\pi} = \{[\varepsilon_k(\Delta^+ + 2m\varepsilon_{k'}) - \varepsilon_k^-(\varepsilon_k - \varepsilon_{k'})^2 c^2\theta]\varepsilon_{k'}^- c\theta' - 2k'\varepsilon_k\varepsilon_{k'} C\theta\} s\theta' c\varphi' - \{(b_-^2 - m\varepsilon_k\Delta^-)c\theta + 2kk'\varepsilon_k\varepsilon_{k'} c\theta'\} s\theta + \varepsilon_k^-\varepsilon_{k'}^-(\varepsilon_k - \varepsilon_{k'})^2 s\theta c\theta s^2\theta' c^2\varphi',$$

$$\frac{\sqrt{2}\kappa_{32}}{\alpha\pi} = \{2k\varepsilon_k\varepsilon_{k'} C\theta' + (b_-^2 - m\varepsilon_k\Delta^-)c\theta\} s\theta + \{[\varepsilon_k(\Delta^+ + 2m\varepsilon_{k'})s^2\theta + (m\Delta^+ + 2\varepsilon_k^2\varepsilon_{k'})c^2\theta]\varepsilon_{k'}^- c\theta' - 2k'\varepsilon_k\varepsilon_{k'} C\theta\} s\theta' c\varphi' + \{[\varepsilon_{k'}(\Delta^+ + 2m\varepsilon_k)s^2\theta' + (m\Delta^+ + 2\varepsilon_k\varepsilon_{k'}^2)(1 + c^2\theta')]\varepsilon_k^- c\theta - 4kk'\varepsilon_k\varepsilon_{k'} c\theta'\} s\theta c^2\varphi',$$

$$\frac{\kappa_{33}}{\alpha\pi} = \{-\varepsilon_{k'}\varepsilon_{k'}[(\Delta^+ - 2m^2)s^2\theta s^2\theta' + 2C\theta C\theta'] - b_-^2 c^2\theta c^2\theta' + m\Delta^-[\varepsilon_{k'} s^2\theta' c^2\theta - \varepsilon_k s^2\theta c^2\theta']\} c\varphi' + [2kk'\varepsilon_k\varepsilon_{k'} + \varepsilon_k^-\varepsilon_{k'}^-(\varepsilon_k - \varepsilon_{k'})^2 c\theta c\theta']\, s\theta s\theta' c^2\varphi',$$

$$\frac{\kappa_{34}}{\alpha\pi} = -\Delta^-\varepsilon_k^- s\theta S\theta' c\theta s^2\varphi',$$

$$\frac{\sqrt{2}\kappa_{41}}{\alpha\pi} = -\Delta^-\{-S\theta(\varepsilon_{k'} - \varepsilon_{k'}^- c^2\theta') + mS\theta' c\varphi' + S\theta s^2\theta'\varepsilon_{k'}^- c^2\varphi'\},$$

$$\frac{\sqrt{2}\kappa_{42}}{\alpha\pi} = \Delta^-\{(\varepsilon_{k'} - \varepsilon_{k'}^- c^2\theta')S\theta + mS\theta' c\varphi' - (\varepsilon_{k'}^+ - \varepsilon_{k'}^- c^2\theta')S\theta c^2\varphi'\},$$

$$\frac{\kappa_{43}}{\alpha\pi} = \Delta^-\varepsilon_{k'}^- s\theta' S\theta c\theta' s^2\varphi',$$

$$\frac{\kappa_{44}}{\alpha\pi} = (-b_-^2 - 2\varepsilon_k\varepsilon_{k'} C\theta C\theta')c\varphi' - \Delta^+ S\theta S\theta' c^2\varphi'.$$

3. Pseudovector

Pseudovector kernels will be given as a sum of the pseudoscalar ones plus a term δ_{ij} which depends on variables t, t' defined in Eq. (98) and vanishes on energy shell ($t=t'=0$):

$$\kappa_{ij} = \kappa_{ij}^{ps} + \delta_{ij}.$$

The following expressions for δ_{ij} are valid only for $x - x' > 0$—with x, x' defined by Eqs. (A2)—and because of this coefficients (A3) are not symmetric in the exchange $(i, k, \theta) \leftrightarrow (i', k', \theta')$. For $x - x' < 0$, the corresponding expressions are obtained by replacing $t \to -t'$, $t' \to -t$ and their symmetry properties are restored.

For $J=0^+$,

$$\frac{\delta_{11}}{\alpha\pi} = m^2\{m^2 tt' + (t - t')\Delta^- - (t + t')(\varepsilon_{k'} C\theta' - \varepsilon_k C\theta)\} - m^2 tt' S\theta S\theta' c\varphi',$$

$$\frac{\delta_{12}}{\alpha\pi} = m\{m^2 tt' + \varepsilon_k^2(t - t') + \varepsilon_k(t + t')C\theta\} S\theta' + m\{m^2 tt' - \varepsilon_{k'}^2(t - t') - \varepsilon_{k'} C\theta'(t + t')\} S\theta c\varphi',$$

$$\frac{\delta_{21}}{\alpha\pi} = m\{m^2 tt' - \varepsilon_{k'}^2(t - t') - \varepsilon_{k'}(t + t')C\theta'\} S\theta + m\{m^2 tt' + \varepsilon_k^2(t - t') + \varepsilon_k(t + t')C\theta\} S\theta' c\varphi',$$

$$\frac{\delta_{22}}{\alpha\pi} = m^2 tt' S\theta S\theta' - m^2[m^2 tt' + (t - t')\Delta^- - (t + t')(\varepsilon_{k'} C\theta' - \varepsilon_k C\theta)]c\varphi'.$$

4. Vector

Vector kernels are written in the form

$$\kappa_{ij} = 2m^2 tt' \frac{m^2}{\mu^2} v_{ij} + \chi_{ij}$$

in which χ_{ij} correspond to the $\mu=0$ case. The v_{ij} contribution, due to μ-dependent term in the vector propagator, appears to be of shell corrections. Positronium kernels are simply given by $\kappa_{ij}^{(PS)} = -\chi_{ij}$.

For $J=0^+$,

$$-\frac{\kappa_{11}}{2\alpha\pi}=2m^2tt'\frac{m^2}{\mu^2}(m^2+S\theta S\theta' c\varphi')+(b_-^2-2\epsilon_{k'}^2\epsilon_k^2),$$

$$-\frac{\kappa_{12}}{2\alpha\pi}=2m^3tt'\frac{m^2}{\mu^2}(S\theta'-S\theta c\varphi')+m\Delta^- S\theta',$$

$$-\frac{\kappa_{21}}{2\alpha\pi}=2m^3tt'\frac{m^2}{\mu^2}(S\theta-S\theta' c\varphi')-m\Delta^- S\theta, \tag{A8}$$

$$-\frac{\kappa_{22}}{2\alpha\pi}=2m^2tt'\frac{m^2}{\mu^2}(S\theta S\theta'+m^2c\varphi')-(\Delta^+S\theta S\theta'+2\epsilon_k\epsilon_{k'}(\epsilon_k\epsilon_{k'}+C\theta C\theta')c\varphi').$$

For $J=1^+$, $a=0$,

$$\frac{\kappa_{11}}{2\alpha\pi}=-2m^2tt'\frac{m^2}{\mu^2}[m^2c\theta c\theta'+\epsilon_k\epsilon_{k'}s\theta s\theta' c\varphi']+[m^2\Delta^+c\theta c\theta'+2\epsilon_k\epsilon_{k'}(kk'+2m^2s\theta s\theta' c\varphi')],$$

$$\frac{\kappa_{12}}{2\alpha\pi}=2m^3tt'\frac{m^2}{\mu^2}[\epsilon_{k'}c\theta s\theta'-\epsilon_k s\theta c\theta' c\varphi']-m\epsilon_{k'}[\Delta^+c\theta s\theta'-2\epsilon_k\epsilon_{k'}s\theta c\theta' c\varphi'],$$

$$\frac{\kappa_{21}}{2\alpha\pi}=2m^3tt'\frac{m^2}{\mu^2}[\epsilon_k s\theta c\theta'-\epsilon_{k'}c\theta s\theta' c\varphi']-m\epsilon_k[\Delta^+s\theta c\theta'-2\epsilon_k\epsilon_{k'}c\theta s\theta' c\varphi'], \tag{A9}$$

$$\frac{\kappa_{22}}{2\alpha\pi}=-2m^2tt'\frac{m^2}{\mu^2}[\epsilon_k\epsilon_{k'}s\theta s\theta'+m^2c\theta c\theta' c\varphi']+[\epsilon_k\epsilon_{k'}\Delta^+s\theta s\theta'+2\epsilon_k\epsilon_{k'}(kk'+\epsilon_k\epsilon_{k'}c\theta c\theta')c\varphi'].$$

For $J=1^+$, $a=1$, the μ-independent kernels χ_{ij} are given by

$$\frac{\chi_{11}}{\alpha\pi}=2\varepsilon_k\varepsilon_{k'}[2C\theta C\theta'+(m\Delta^+\varepsilon_{k'}\varepsilon_k^-c^2\theta+\varepsilon_k\varepsilon_{k'}^-c^2\theta')]+[4kk'\varepsilon_k\varepsilon_{k'}+\Delta^+(kk'+\varepsilon_k^-\varepsilon_{k'}^-)]s\theta s\theta' c\varphi'+2\varepsilon_k\varepsilon_{k'}\varepsilon_k^-\varepsilon_{k'}^-s^2\theta s^2\theta' c^2\varphi',$$

$$\frac{\chi_{12}}{\alpha\pi}=[kk'(4\varepsilon_k\varepsilon_{k'}-\Delta^+)+\varepsilon_k^-\varepsilon_{k'}^-\Delta^+c\theta c\theta']s\theta s\theta' c\varphi'-2\varepsilon_k\varepsilon_{k'}\varepsilon_k^-(2\varepsilon_{k'}-\varepsilon_{k'}^-s^2\theta')s^2\theta c^2\varphi'+2\varepsilon_k\varepsilon_{k'}[\varepsilon_k\varepsilon_{k'}(c^2\theta'-c^2\theta)+m(\varepsilon_k s^2\theta'-\varepsilon_{k'}s^2\theta)],$$

$$\frac{\chi_{13}}{\sqrt{2}\alpha\pi}=-2\varepsilon_k\varepsilon_{k'}(kk'c\theta+\varepsilon_k\varepsilon_{k'}^-c\theta')s\theta'-\{\varepsilon_k^-\Delta^+(m+\varepsilon_{k'}^-s^2\theta')c\theta-4kk'\varepsilon_k\varepsilon_{k'}c\theta'\}s\theta c\varphi'+2\varepsilon_k\varepsilon_{k'}\varepsilon_k^-\varepsilon_{k'}^-s^2\theta s\theta' c\theta' c^2\varphi',$$

$$\frac{\chi_{14}}{\sqrt{2}\alpha\pi}=m\Delta^-S\theta c\varphi',$$

$$\frac{\chi_{21}}{\alpha\pi}=[kk'(4\varepsilon_k\varepsilon_{k'}-\Delta^+)+\varepsilon_k^-\varepsilon_{k'}^-\Delta^+c\theta c\theta']s\theta s\theta' c\varphi'-2\varepsilon_k\varepsilon_{k'}\varepsilon_{k'}^-(2\varepsilon_k-\varepsilon_k^-s^2\theta)s^2\theta' c^2\varphi'-2\varepsilon_k\varepsilon_{k'}[\varepsilon_k\varepsilon_{k'}(c^2\theta'-c^2\theta)+m(\varepsilon_k s^2\theta'-\varepsilon_{k'}s^2\theta)],$$

$$\frac{\chi_{22}}{\alpha\pi}=-2\varepsilon_k\varepsilon_{k'}\{m(\varepsilon_k+\varepsilon_{k'})+\varepsilon_k\varepsilon_{k'}^-c^2\theta'+\varepsilon_{k'}\varepsilon_k^-c^2\theta+2C\theta C\theta'\}+\{kk'(4\varepsilon_k\varepsilon_{k'}+\Delta^+)+\varepsilon_k^-\varepsilon_{k'}^-\Delta^+c\theta c\theta'\}s\theta s\theta' c\varphi'+2\varepsilon_k\varepsilon_{k'}\{(\varepsilon_{k'}^++\varepsilon_{k'}^-c^2\theta')(\varepsilon_k^++\varepsilon_k^-c^2\theta)+4C\theta C\theta'\}c^2\varphi',$$

$$\frac{\chi_{23}}{\sqrt{2}\alpha\pi}=2\varepsilon_k\varepsilon_{k'}(kk'c\theta+\varepsilon_{k'}^-\varepsilon_k c\theta')s\theta'-2\varepsilon_k\varepsilon_{k'}\{2kk'c\theta+(\varepsilon_k^++\varepsilon_k^-c^2\theta)\varepsilon_{k'}^-c\theta'\}s\theta' c^2\varphi'+\{4kk'\varepsilon_k\varepsilon_{k'}c\theta'-\varepsilon_k^-\Delta^+(m+\varepsilon_{k'}^-s^2\theta')c\theta\}s\theta c\varphi',$$

$$\frac{\chi_{24}}{\sqrt{2}\alpha\pi}=-m\Delta^-S\theta c\varphi',$$

$$\frac{\chi_{31}}{\sqrt{2}\alpha\pi}=-2\varepsilon_k\varepsilon_{k'}(kk'c\theta'+\varepsilon_{k'}\varepsilon_k^-c\theta)s\theta-\{\varepsilon_{k'}^-\Delta^+(m+\varepsilon_k^-s^2\theta)c\theta'-4kk'\varepsilon_k\varepsilon_{k'}c\theta\}s\theta' c\varphi'+2\varepsilon_k\varepsilon_{k'}\varepsilon_k^-\varepsilon_{k'}^-c\theta s\theta s^2\theta' c^2\varphi',$$

$$\frac{\chi_{32}}{\sqrt{2}\alpha\pi}=2\varepsilon_k\varepsilon_{k'}(kk'c\theta'+\varepsilon_k^-\varepsilon_{k'}c\theta)s\theta-2\varepsilon_k\varepsilon_{k'}\{2kk'c\theta'+(\varepsilon_{k'}^++\varepsilon_{k'}^-c^2\theta')\varepsilon_k^-c\theta\}s\theta c^2\varphi'+\{4kk'\varepsilon_k\varepsilon_{k'}c\theta-\varepsilon_{k'}^-\Delta^+(m+\varepsilon_k^-s^2\theta)c\theta'\}s\theta' c\varphi',$$

$$\frac{\chi_{33}}{\alpha\pi}=4\varepsilon_k\varepsilon_{k'}(kk'+\varepsilon_k^-\varepsilon_{k'}^-)s\theta s\theta' c^2\varphi'+2\{4\varepsilon_k\varepsilon_{k'}C\theta C\theta'+\Delta^+(\varepsilon_k\varepsilon_{k'}+\varepsilon_k^-\varepsilon_{k'}^-c^2\theta c^2\theta'-\varepsilon_{k'}\varepsilon_k^-c^2\theta-\varepsilon_k\varepsilon_{k'}^-c^2\theta')\}c\varphi',$$

$$\frac{\chi_{34}}{\alpha\pi}=0,$$

$$\frac{\chi_{41}}{\sqrt{2}\alpha\pi} = -m\Delta^- S\theta' c\varphi',$$

$$\frac{\chi_{42}}{\alpha\pi} = m\Delta^- S\theta' c\varphi',$$

$$\frac{\chi_{43}}{\alpha\pi} = 0,$$

$$\frac{\chi_{44}}{\alpha\pi} = 2(2\varepsilon_k^2\varepsilon_{k'}^2 - b_-^2)c\varphi'$$

and the v_{ij} contribution reads

$$\frac{v_{11}}{\alpha\pi} = m[\varepsilon_k^- c^2\theta + \varepsilon_{k'}^- c^2\theta' - (\varepsilon_k + \varepsilon_{k'})] - [kk' + \varepsilon_k^-\varepsilon_{k'}^- c\theta c\theta']s\theta s\theta' c\varphi' - \varepsilon_k^-\varepsilon_{k'}^- s^2\theta s^2\theta' c^2\varphi',$$

$$\frac{v_{12}}{\alpha\pi} = m[(\varepsilon_k - \varepsilon_{k'}) - \varepsilon_k^- c^2\theta + \varepsilon_{k'}^- c^2\theta'] + [kk' - \varepsilon_k^-\varepsilon_{k'}^- c\theta c\theta']s\theta s\theta' c\varphi' - \varepsilon_k^-(\varepsilon_{k'}^+ - \varepsilon_{k'}^- c^2\theta')s^2\theta c^2\varphi',$$

$$\frac{v_{13}}{\sqrt{2}\alpha\pi} = -m\varepsilon_{k'}^- s\theta' c\theta' + \varepsilon_k^-(m + \varepsilon_{k'}^- s^2\theta')s\theta c\theta c\varphi' - \varepsilon_k^-\varepsilon_{k'}^- s^2\theta s\theta' c\theta' c^2\varphi',$$

$$\frac{v_{14}}{\sqrt{2}\alpha\pi} = (m + \varepsilon_k^- s^2\theta)S\theta' - mS\theta c\varphi' - \varepsilon_k^- s^2\theta S\theta' c^2\varphi',$$

$$\frac{v_{21}}{\alpha\pi} = -m[(\varepsilon_k - \varepsilon_{k'}) + \varepsilon_{k'}^- c^2\theta' - \varepsilon_k^- c^2\theta] + [kk' - \varepsilon_k^-\varepsilon_{k'}^- c\theta c\theta']s\theta s\theta' c\varphi' - \varepsilon_{k'}^-(\varepsilon_k^+ - \varepsilon_{k'}^- c^2\theta)s^2\theta' c^2\varphi',$$

$$\frac{v_{22}}{\alpha\pi} = m[(\varepsilon_k + \varepsilon_{k'}) - \varepsilon_k^- c^2\theta - \varepsilon_{k'}^- c^2\theta'] - (kk' + \varepsilon_k^-\varepsilon_{k'}^- c\theta c\theta')s\theta s\theta' c\varphi' - (2m + \varepsilon_k^- s^2\theta)(2m + \varepsilon_{k'}^- s^2\theta')c^2\varphi',$$

$$\frac{v_{23}}{\sqrt{2}\alpha\pi} = m\varepsilon_{k'}^- s\theta' c\theta' + \varepsilon_k^- s\theta c\theta(m + \varepsilon_{k'}^- s^2\theta')c\varphi' - \varepsilon_{k'}^-(\varepsilon_k^+ - \varepsilon_k^- c^2\theta)s\theta' c\theta' c^2\varphi',$$

$$\frac{v_{24}}{\sqrt{2}\alpha\pi} = (m + \varepsilon_k^- s^2\theta)S\theta' + mS\theta c\varphi' - (2m + \varepsilon_k^- s^2\theta)S\theta' c^2\varphi',$$

$$\frac{v_{31}}{\sqrt{2}\alpha\pi} = -m\varepsilon_k^- s\theta c\theta + \varepsilon_{k'}^-(m + \varepsilon_k^- s^2\theta)s\theta' c\theta' c\varphi' - \varepsilon_k^-\varepsilon_{k'}^- s^2\theta' s\theta c\theta c^2\varphi',$$

$$\frac{v_{32}}{\sqrt{2}\alpha\pi} = m\varepsilon_k^- s\theta c\theta + \varepsilon_{k'}^- s\theta' c\theta'(m + \varepsilon_k^- s^2\theta)c\varphi' - \varepsilon_k^-(\varepsilon_{k'}^+ - \varepsilon_{k'}^- c^2\theta')s\theta c\theta c^2\varphi',$$

$$\frac{v_{33}}{\alpha\pi} = -2(m + \varepsilon_{k'}^- s^2\theta')(m + \varepsilon_k^- s^2\theta)c\varphi' - 2\varepsilon_k^-\varepsilon_{k'}^- c\theta c\theta' s\theta s\theta' c^2\varphi',$$

$$\frac{v_{34}}{\alpha\pi} = 2\varepsilon_k^- s\theta c\theta S\theta' s^2\varphi',$$

$$\frac{v_{41}}{\sqrt{2}\alpha\pi} = (m + \varepsilon_{k'}^- s^2\theta')S\theta - mS\theta' c\varphi' - \varepsilon_{k'}^- S\theta s^2\theta' c^2\varphi',$$

$$\frac{v_{42}}{\alpha\pi} = (m + \varepsilon_{k'}^- s^2\theta')S\theta + mS\theta' c\varphi' - (2m + \varepsilon_{k'}^- s^2\theta')S\theta c^2\varphi',$$

$$\frac{v_{43}}{\alpha\pi} = 2\varepsilon_{k'}^- s\theta' c\theta' S\theta s^2\varphi',$$

$$\frac{v_{44}}{\alpha\pi} = -2(m^2 + S\theta S\theta' c\varphi')c\varphi'.$$

APPENDIX B: RELATIONS BETWEEN THE COMPONENTS OF $J=1$ STATE

The wave function of the $J=1$ state is represented in two forms: in form (49) with the components φ_i and in form (51) with the components f_i. The formulas expressing the components φ_i in terms of the f_i, in approximation $M \approx 2m$, are given in Appendix C from Ref. [57]. Here we give these relations for arbitrary M (note that φ_3 and φ_6 only differ relative to Ref. [57]; we denote below $z=\cos\theta$):

$$\varphi_1 = \frac{m^2(2\varepsilon_k + m)}{4\varepsilon_k k^2} f_2 + \frac{m^2}{4\varepsilon_k(\varepsilon_k + m)}(\sqrt{2}f_1 - f_3 + zf_4 - \sqrt{3}zf_6),$$

$$\varphi_2 = \frac{m}{4\varepsilon_k}(\sqrt{2}f_1 - f_2 - f_3 - 2zf_4),$$

$$\varphi_3 = -\frac{\sqrt{2}(2\varepsilon_k - M)^2 k}{16\varepsilon_k^2(\varepsilon_k + m)} z f_1 - \frac{(2\varepsilon_k + m)(2\varepsilon_k - M)^2}{16\varepsilon_k^2 k} z f_2 + \frac{(4\varepsilon_k^2 + 8M\varepsilon_k + M^2)k}{16\varepsilon_k^2(\varepsilon_k + m)} z f_3 + \frac{3M}{4k}\left(1 - \frac{z^2(2\varepsilon_k - M)^2 k^2}{12M\varepsilon_k^2(\varepsilon_k + m)}\right) f_4 + \frac{\sqrt{3}M}{4k}\left(1 + \frac{z^2(2\varepsilon_k - M)^2 k^2}{4M\varepsilon_k^2(\varepsilon_k + m)}\right) f_6,$$

$$\varphi_4 = -\frac{3m}{2k} f_4 + \frac{\sqrt{3}m}{2k} f_6,$$

$$\varphi_5 = \frac{1}{2}\sqrt{\frac{3}{2}}\frac{m^2}{k\varepsilon_k} f_5,$$

$$\varphi_6 = \frac{(2\varepsilon_k - M)^2}{8m\varepsilon_k}(\sqrt{2} f_1 - f_2 + z f_4 - \sqrt{3} z f_6) - \frac{(4\varepsilon_k^2 + 8M\varepsilon_k + M^2)}{8m\varepsilon_k} f_3. \quad \text{(B1)}$$

The state with $J=1, a=1$ is determined by Eq. (67) as a decomposition in four orthogonal spin structures $S_{i\mu}^{(1)}$. These four structures are expressed by Eq. (68) in terms of six structures $S_{j\mu}$, defined in Eq. (48), with the coefficients h_{ij} given below. These coefficients are found as follows. We substitute formulas (66) into Eqs. (B1) and then Eqs. (B1) into Eq. (49). In this way the wave function $\phi_\mu^{(1)}$ is expressed in terms of the four functions $g_i^{(1)}$, i.e., obtains the form (67). The coefficients at the front of $g_i^{(1)}$ are the structures $S_{i\mu}^{(1)}$. Collecting these coefficients, we find $S_{i\mu}^{(1)}$ in terms of six structures $S_{j\mu}$, in the form of Eq. (68) with the following coefficients h_{ij}:

$$h_{11} = \frac{\sqrt{3}m^2}{4\varepsilon_k(\varepsilon_k + m)}, \quad h_{12} = \frac{\sqrt{3}m}{4\varepsilon_k},$$

$$h_{13} = -\frac{\sqrt{3}(\varepsilon_k - m)(4\varepsilon_k^2 + M^2)z}{16\varepsilon_k^2 k},$$

$$h_{14} = h_{15} = 0, \quad h_{16} = \frac{\sqrt{3}(4\varepsilon_k^2 + M^2)}{8\varepsilon_k m},$$

$$h_{21} = \frac{\sqrt{3}m^2[\varepsilon_k(1 - z^2) + m(1 + z^2)]}{4\varepsilon_k k^2(1 - z^2)}, \quad h_{22} = -\frac{\sqrt{3}m}{4\varepsilon_k},$$

$$h_{23} = -\frac{\sqrt{3}(4\varepsilon_k^2 + M^2)[\varepsilon_k(1 - z^2) + m(1 + z^2)]z}{16\varepsilon_k^2 k(1 - z^2)},$$

$$h_{24} = \frac{\sqrt{3}mz}{k(1 - z^2)},$$

$$h_{25} = 0, \quad h_{26} = -\frac{\sqrt{3}(4\varepsilon_k^2 + M^2)(1 + z^2)}{8\varepsilon_k m(1 - z^2)},$$

$$h_{31} = \frac{\sqrt{3}m^2 z}{2\varepsilon_k(\varepsilon_k + m)\sqrt{2(1 - z^2)}}, \quad h_{32} = 0,$$

$$h_{33} = -\frac{\sqrt{3}(\varepsilon_k - m)(4\varepsilon_k^2 + M^2)z^2}{8\varepsilon_k^2 k\sqrt{2(1 - z^2)}},$$

$$h_{34} = -\frac{\sqrt{3}m}{k\sqrt{2(1 - z^2)}}, \quad h_{35} = 0,$$

$$h_{36} = \frac{\sqrt{3}(4\varepsilon_k^2 + M^2)z}{4\varepsilon_k m\sqrt{2(1 - z^2)}},$$

$$h_{41} = h_{42} = h_{43} = h_{44} = 0, \quad h_{45} = \frac{\sqrt{3}m^2}{2\varepsilon_k k\sqrt{2(1 - z^2)}},$$

$$h_{46} = 0. \quad \text{(B2)}$$

[1] The so-called Klein-Gordon equation with the many fathers: O. Klein, Z. Phys. **37**, 895 (1926); V. Fock, *ibid.* **38**, 242 (1926); **39**, 226 (1926); E. Schrodinger, Ann. Phys. **81**, 109 (1926); J. Kudar, *ibid.* **81**, 632 (1926); W. Gordon, Z. Phys. **40**, 117 (1926); Th. de Donder and H. Van Dungen, C. R. **183**, 22 (1926). See, for instance, H. Kragh, Am. J. Phys. **52**, 1024 (1984) for a historical review.

[2] P. A. M. Dirac, Proc. R. Soc. London, Ser. A **117**, 610 (1928).

[3] C. Bochna *et al.*, Phys. Rev. Lett. **81**, 4576 (1998).

[4] L. C. Alexa *et al.*, Phys. Rev. Lett. **82**, 1374 (1999).

[5] D. Abbott *et al.*, Phys. Rev. Lett. **82**, 1379 (1999).

[6] D. Abbott *et al.*, Phys. Rev. Lett. **84**, 5053 (2000).

[7] M. Garcon and J. W. Van Orden, Adv. Nucl. Phys. **26**, 293 (2001); nucl-th/0102049.

[8] R. Gilman and F. Gross, J. Phys. G **28**, R37 (2002); nucl-th/0111015.

[9] E. E. Salpeter and H. A. Bethe, Phys. Rev. **84**, 1232 (1951).

[10] J. Fleischer and J. A. Tjon, Phys. Rev. D **21**, 87 (1980).

[11] M. J. Zuilhof and J. A. Tjon, Phys. Rev. C **22**, 2369 (1980).

[12] E. E. van Faassen and J. A. Tjon, Phys. Rev. C **33**, 2105 (1986).

[13] G. Rupp and J. A. Tjon, Phys. Rev. C **45**, 2133 (1992).

[14] D. R. Phillips and I. R. Afnan, Phys. Rev. C **54**, 1542 (1992).

[15] S. G. Bondarenko *et al.*, Prog. Part. Nucl. Phys. **48**, 449 (2002).

[16] A. A. Logunov and A. N. Tavkhelidze, Nuovo Cimento **29**, 370 (1963).

[17] R. Blankenbecler and R. Sugar, Phys. Rev. **142**, 1951 (1966).

[18] F. Gross, Phys. Rev. **186**, 1448 (1969); Phys. Rev. D **10**, 223 (1974); Phys. Rev. C **26**, 2203 (1982).

[19] W. Buck and F. Gross, Phys. Lett. **63**, 286 (1976); Phys. Rev. D **20**, 2361 (1979); G. Arnold, C. E. Carlson, and F. Gross, Phys. Rev. C **21**, 1426 (1980); F. Gross, J. W. Van Orden, and K. Holinde, *ibid.* **45**, 2094 (1992).

[20] D. R. Phillips and S. J. Wallace, Phys. Rev. C **54**, 507 (1996); Few-Body Syst. **24**, 175 (1998); P. C. Dulany and S. J. Wal-

lace, Phys. Rev. C **56**, 2992 (1997); D. R. Phillips, S. J. Wallace, and N. K. Devine, *ibid.* **58**, 2261 (1998).
[21] E. Hummel and J. A. Tjon, Phys. Rev. C **42**, 423 (1990).
[22] P. A. M. Dirac, Rev. Mod. Phys. **21**, 392 (1949).
[23] H. Leutwyler and J. Stern, Ann. Phys. **112**, 94 (1978).
[24] P. L. Chung, F. Coester, B. D. Keister, and W. N. Polyzou, Phys. Rev. C **37**, 2000 (1988).
[25] F. Coester, Prog. Part. Nucl. Phys. **29**, 1 (1992).
[26] M. G. Fuda, Ann. Phys. (N.Y.) **197**, 265 (1990); **231**, 1 (1994); Nucl. Phys. **A543**, 111c (1992).
[27] M. G. Fuda and Y. Zhang, Phys. Rev. C **51**, 23 (1995).
[28] Ch.-R. Ji, Phys. Lett. B **322**, 389 (1994).
[29] M. Burkardt, Adv. Nucl. Phys. **23**, 1 (1996).
[30] B. L. Bakker, L. A. Kondratyuk, and M. V. Terentev, Nucl. Phys. **B158**, 497 (1979).
[31] N. E. Ligterink and B. L. G. Bakker, Phys. Rev. D **52**, 5954 (1995).
[32] N. C. J. Schoonderwoerd and B. L. G. Bakker, Phys. Rev. D **58**, 025013 (1998).
[33] N. Schoonderwoerd, B. L. G. Bakker, and V. A. Karmanov, Phys. Rev. C **58**, 3093 (1998).
[34] J. R. Hiller, Nucl. Phys. **B90**, 170 (2000).
[35] B. D. Keister and W. N. Polyzou, Adv. Nucl. Phys. **20**, 225 (1991).
[36] S. J. Brodsky, H.-C. Pauli, and S. S. Pinsky, Phys. Rep. **301**, 299 (1998).
[37] M. Kraugartner, H. C. Pauli, and F. Wolz, Phys. Rev. D **45**, 3755 (1992).
[38] U. Trittmann and H.-C. Pauli, Nucl. Phys. B, Proc. Suppl. **90**, 161 (2000).
[39] Uwe Trittmann, Int. J. Mod. Phys. A **16S1C**, 987 (2001).
[40] T. Frederico and H.-C. Pauli, Phys. Rev. D **D64**, 054007 (2001).
[41] T. Frederico, H.-C. Pauli, and S.-G. Zhou, Phys. Rev. D **66**, 054007 (2002).
[42] G. A. Miller, Prog. Part. Nucl. Phys. **45**, 83 (2000).
[43] G. A. Miller and R. Machleidt, Phys. Rev. C **60**, 035202 (1999); nucl-th/9903080.
[44] J. R. Cooke, G. A. Miller, and D. R. Phillips, Phys. Rev. C **61**, 064005 (2000); nucl-th/9910013.
[45] J. R. Cooke and G. A. Miller, Phys. Rev. C **66**, 034002 (2002).
[46] St. Glazek, A. Harindranath, S. Pinsky, J. Shigemutsu, and K. Wilson, Phys. Rev. D **47**, 1599 (1993).
[47] J. H. O. Sales, T. Frederico, B. V. Carlson, and P. U. Sauer, Phys. Rev. C **61**, 04003 (2000).
[48] L. L. Frankfurt, M. I. Strikman, L. Mankiewicz, and M. Sawicki, Few-Body Syst. **8**, 37 (1990).
[49] M. M. Gianini, L. Kondratyuk, and P. Saracco, Few-Body Syst. **17**, 21 (1994).
[50] H. J. Weber, Ann. Phys. **207**, 417 (1991).
[51] F. Cardarelli, I. L. Grach, I. M. Narodetskii, G. Salme, and S. Simula, Phys. Lett. B **349**, 393 (1995).
[52] *Proceedings of the Tenth Light-Cone Meeting*, Heidelberg, 2000, edited by H. C. Pauli *et al.* [Nucl. Phys. B Proc. Suppl. 90 (2000)].
[53] *Proceedings of the 11th Light-Cone Meeting*, Trento, 2001, edited by A. Bassetto *et al.*, Nucl. Phys. B Proc. Suppl 108, (2002).
[54] V. A. Karmanov, Zh. Eksp. Teor. Fiz. **71**, 399 (1976) [JETP **44**, 210 (1976)].
[55] V. A. Karmanov, Nucl. Phys. **B166**, 378 (1980).
[56] V. A. Karmanov, Nucl. Phys. **A362**, 331 (1981).
[57] J. Carbonell, B. Desplanques, V. A. Karmanov, and J. F. Mathiot, Phys. Rep. **300**, 215 (1998).
[58] J. Carbonell and V. A. Karmanov, Nucl. Phys. **A581**, 625 (1995).
[59] J. Carbonell and V. A. Karmanov, Nucl. Phys. **A589**, 713 (1995).
[60] R. Machleidt, K. Holinde, and C. Elster, Phys. Rep. **149**, 1 (1987).
[61] J. Carbonell and V. A. Karmanov, Eur. Phys. J. A **6**, 9 (1999).
[62] A. N. Antonov, M. Gaidarov, M. V. Ivanov, D. N. Kadrev, G. Z. Krumova, P. E. Hodgson, and H. V. von Geramb, Phys. Rev. C **65**, 024306 (2002); nucl-th/0106044.
[63] M. K. Gaidarov, M. V. Ivanov, and A. N. Antonov, nucl-th/0207081.
[64] M. Mangin-Brinet and J. Carbonell, Phys. Lett. B **474**, 237 (2000).
[65] M. Mangin-Brinet, J. Carbonell, and V. A. Karmanov, Nucl. Phys. **B90**, 123 (2000).
[66] V. A. Karmanov, J. Carbonell, and M. Mangin-Brinet, Nucl. Phys. **A684**, 366c (2001).
[67] M. Mangin-Brinet and J. Carbonell, Nucl. Phys. **A689**, 463c (2001).
[68] M. Mangin-Brinet, J. Carbonell, and V. A. Karmanov, Phys. Rev. D **64**, 027701 (2001); **64**, 125005 (2001). We noticed a misprint in κ_{12}, κ_{32}, κ_{41} of the $J=1$, $a=1$ kernel given in Appendix A, and it is now corrected.
[69] V. A. Karmanov, J. Carbonell, and M. Mangin-Brinet, in *Mesons and Light Nuclei*, edited by Petr Bydz Ovsky and Jirí Mares, AIP Conf. Proc. No. 603 (AIP, Melville, NY, 2001), pp. 271–274; hep-th/0107237.
[70] V. A. Karmanov, J. Carbonell, and M. Mangin-Brinet, Nucl. Phys. B, Proc. Suppl. **108**, 256 (2002); nucl-th/0112005.
[71] M. Mangin-Brinet, J. Carbonell, and V. A. Karmanov, Nucl. Phys. B, Proc. Suppl. **108**, 259 (2002); hep-th/0112017.
[72] M. Mangin-Brinet, Thèse, Université de Paris VII, 2001.
[73] J. Carbonell and V. A. Karmanov, Phys. Rev. C **67**, 037001 (2003).
[74] J. Carbonell, M. Mangin-Brinet, and V. A. Karmanov, nucl-th/0202042.
[75] V. A. Karmanov and J. Carbonell, nucl-th/0207075.
[76] G. C. Wick, Phys. Rev. **96**, 1124 (1954); R. E. Cutkosky, *ibid.* **96**, 1135 (1954).
[77] V. G. Kadyshevsky, Zh. Eksp. Teor. Fiz. **46**, 645 (1964) [JETP **19**, 443 (1964)]; Zh. Eksp. Teor. Fiz. **46**, 872 (1964) [JETP **19**, 597 (1964)]; Nucl. Phys. **B6**, 125 (1968).
[78] V. A. Karmanov, Zh. Eksp. Teor. Fiz. **83**, 3 (1982) [JETP **56**, 1 (1982)].
[79] H. A. Bethe and E. E. Salpeter, *Quantum Mechanics of One- and Two-Electron Atoms* (Plenum, New York, 1977).
[80] E. Epelbaum, W. Glockle, and U. G. Meissner, Nucl. Phys. **A671**, 295 (2000).